2010-12

Torque control of a separate excitation DC motor for a dynamometer

Derges, Jonathan R.

Monterey, California. Naval Postgraduate School

NAVAL POSTGRADUATE SCHOOL

MONTEREY, CALIFORNIA

THESIS

TORQUE CONTROL OF A SEPARATE-WINDING EXCITATION DC MOTOR FOR A DYNAMOMETER

by

Jonathan R. Derges

December 2010

Thesis Advisor:	Alexander L. Julian
Second Reader:	Roberto Cristi

Approved for public release; distribution is unlimited

THIS PAGE INTENTIONALLY LEFT BLANK

REPORT DOCUMENTATION PAGE			Form Approved OMB No. 0704-0188
Public reporting burden for this collection of information is estimated to average 1 hour per response, including the time for reviewing instruction, searching existing data sources, gathering and maintaining the data needed, and completing and reviewing the collection of information. Send comments regarding this burden estimate or any other aspect of this collection of information, including suggestions for reducing this burden, to Washington headquarters Services, Directorate for Information Operations and Reports, 1215 Jefferson Davis Highway, Suite 1204, Arlington, VA 22202-4302, and to the Office of Management and Budget, Paperwork Reduction Project (0704-0188) Washington DC 20503.			
1. AGENCY USE ONLY ***(Leave blank)***	**2. REPORT DATE** December 2010	**3. REPORT TYPE AND DATES COVERED** Master's Thesis	
4. TITLE AND SUBTITLE Torque Control of a Separate-Winding Excitation DC Motor for a Dynamometer		**5. FUNDING NUMBERS**	
6. AUTHOR(S) Jonathan R. Derges			
7. PERFORMING ORGANIZATION NAME(S) AND ADDRESS(ES) Naval Postgraduate School Monterey, CA 93943-5000		**8. PERFORMING ORGANIZATION REPORT NUMBER**	
9. SPONSORING /MONITORING AGENCY NAME(S) AND ADDRESS(ES) N/A		**10. SPONSORING/MONITORING AGENCY REPORT NUMBER**	
11. SUPPLEMENTARY NOTES The views expressed in this thesis are those of the author and do not reflect the official policy or position of the Department of Defense or the U.S. Government. IRB Protocol number: N/A.			
12a. DISTRIBUTION / AVAILABILITY STATEMENT Approved for public release; distribution is unlimited		**12b. DISTRIBUTION CODE** A	

13. ABSTRACT

In this thesis, the theory behind a separate-winding excitation direct current (DC) motor and profile of the motor's torque versus rotor speed is studied. The torque versus rotor speed profile results are predictably linear at a given armature voltage.

Output torque of a separate-winding excitation DC motor is proportional to the armature current. From this theory, a program was written in Simulink with Xilinx embedded software to enable a user to command the DC motor torque through a Graphical User Interface (GUI). The command is then converted to control armature current through a Field Programmable Gate Array (FPGA) to the DC motor. The armature current level is maintained through a programmed Proportional Integral (PI) Controller to keep output torque constant regardless of armature voltage and rotor speed. This result is a way to command constant output torque to a DC motor.

14. SUBJECT TERMS Direct Current (DC) motor, Programmable Gate Array (FPGA), Proportional Integral (PI) Controller, Torque, Rotor Speed			**15. NUMBER OF PAGES** 77
			16. PRICE CODE
17. SECURITY CLASSIFICATION OF REPORT Unclassified	**18. SECURITY CLASSIFICATION OF THIS PAGE** Unclassified	**19. SECURITY CLASSIFICATION OF ABSTRACT** Unclassified	**20. LIMITATION OF ABSTRACT** UU

NSN 7540-01-280-5500

Standard Form 298 (Rev. 2-89)
Prescribed by ANSI Std. 239-18

THIS PAGE INTENTIONALLY LEFT BLANK

Approved for public release; distribution is unlimited

TORQUE CONTROL OF A SEPARATE EXCITATION DC MOTOR FOR A DYNAMOMETER

Jonathan R. Derges
Lieutenant, United States Navy
B.S., Old Dominion University, 2004

Submitted in partial fulfillment of the
requirements for the degree of

MASTER OF SCIENCE IN ELECTRICAL ENGINEERING

from the

NAVAL POSTGRADUATE SCHOOL
December 2010

Author: Jonathan R. Derges

Approved by: Alexander L. Julian
Thesis Advisor

Roberto Cristi
Second Reader

R. Clark Robertson
Chairman, Department of Electrical and Computer Engineering

THIS PAGE INTENTIONALLY LEFT BLANK

ABSTRACT

In this thesis, the theory behind a separate-winding excitation direct current (DC) motor and profile of the motor's torque versus rotor speed is studied. The torque versus rotor speed profile results are predictably linear at a given armature voltage.

Output torque of a separate-winding excitation DC motor is proportional to the armature current. From this theory, a program was written in Simulink with Xilinx embedded software to enable a user to command the DC motor torque through a Graphical User Interface (GUI). The command is then converted to control armature current through a Field Programmable Gate Array (FPGA) to the DC motor. The armature current level is maintained through a programmed Proportional Integral (PI) Controller to keep output torque constant regardless of armature voltage and rotor speed. This result is a way to command constant output torque to a DC motor.

THIS PAGE INTENTIONALLY LEFT BLANK

TABLE OF CONTENTS

LIST OF FIGURES

THIS PAGE INTENTIONALLY LEFT BLANK

LIST OF TABLES

THIS PAGE INTENTIONALLY LEFT BLANK

EXECUTIVE SUMMARY

The research completed in this thesis investigates the theory behind separate-winding excitation DC motor operation in order to design a way to command and control torque through a user interface. Previous research on a doubly-fed induction generator (DFIG) control system that uses a DC motor to provided variable input torque did not offer an accurate means of providing specifically defined input torque.

There are a many different ways to operate a DC motor. The basic separate-winding excitation setup was selected because of its ease and known predictability. A separate-winding excitation DC motor was step up and tested. The figure below shows the how the DC motor behaved in regards to the motor's output electric torque versus rotational speed at a given armature voltage (V_A).

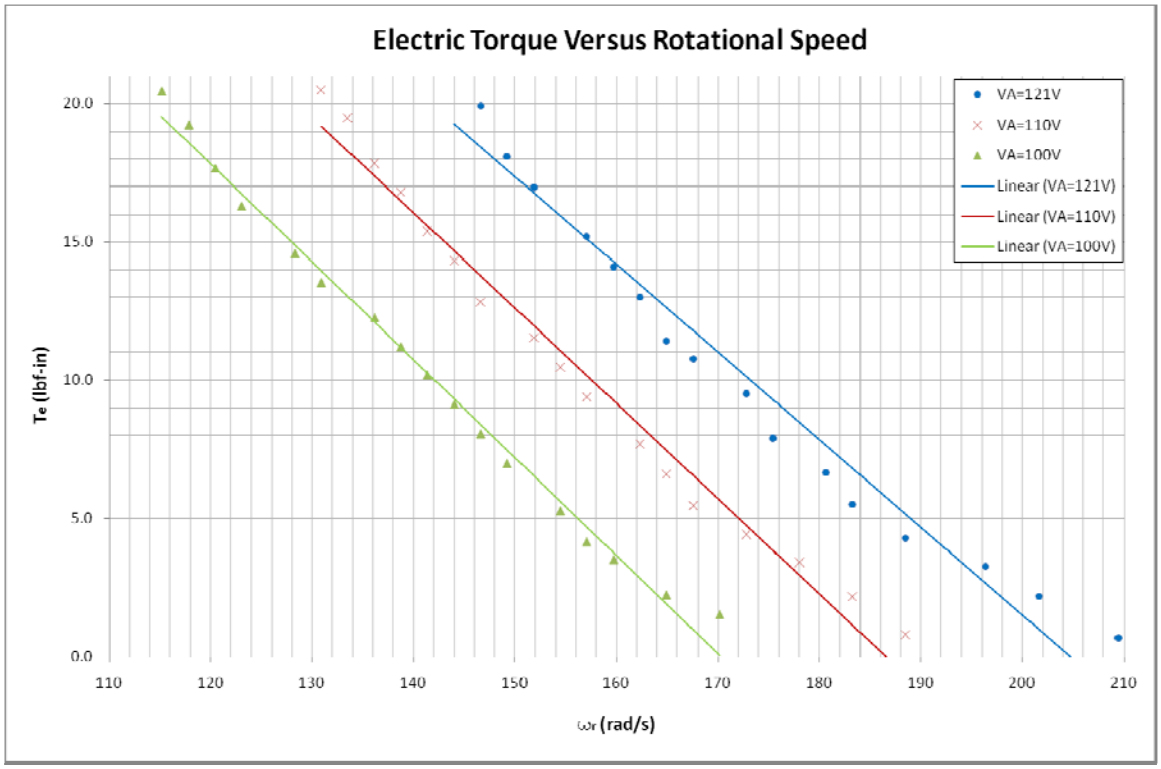

Electric torque versus rotational speed for a separate-winding excitation DC motor

A program was written in Matlab/Simulink software with Xilinx embedded software that uses a Field Programmable Gate Array (FPGA) system to operate the DC motor. Using the theory validated on the separate-winding excitation operational setup, we wrote a program to take a user defined torque combined with the measured rotor speed to provide the correct armature voltage to the DC motor. However, the program did not initially work because the program was written for constant rotor speed and user defined torque. When load was applied to the DC motor, the rotor speed changes, and consequently, the armature voltage and current changes. By having varying armature current, the motor had varying output torque.

From DC motor theory, output torque is also directly proportional to armature current (I_a). From this theory, the program was altered to take the user defined torque and apply the correct armature current to the DC motor. The armature current was also stabilized through a PI controller to keep the average, armature current constant and, therefore, keep the output torque constant regardless of rotational speed and load variations. The following two figures show constant armature current on channel 3 at different speeds and armature voltages.

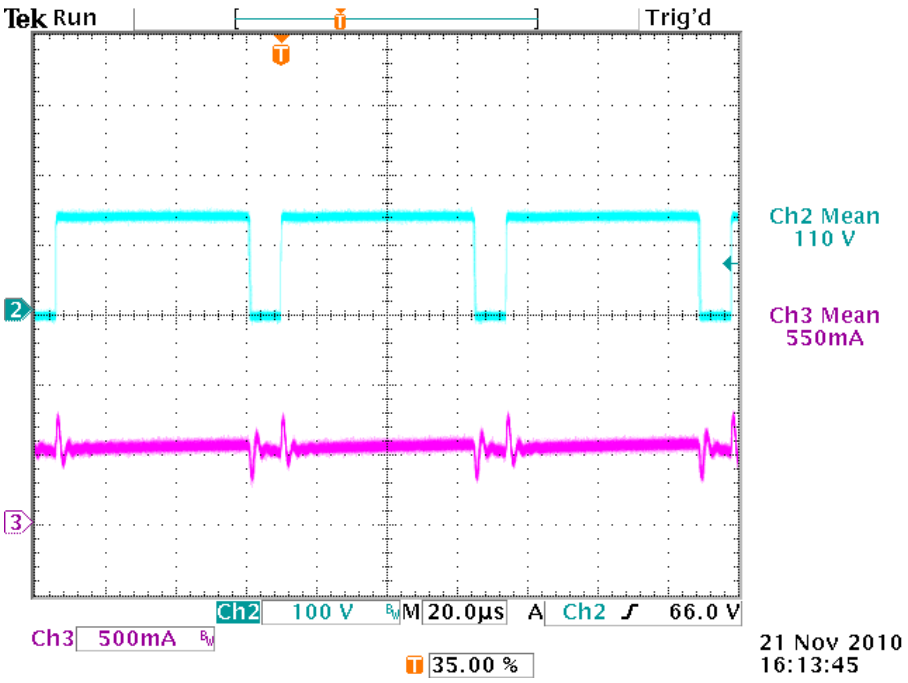

Armature voltage and current at 4 lbf-in commanded and 1900 rpm

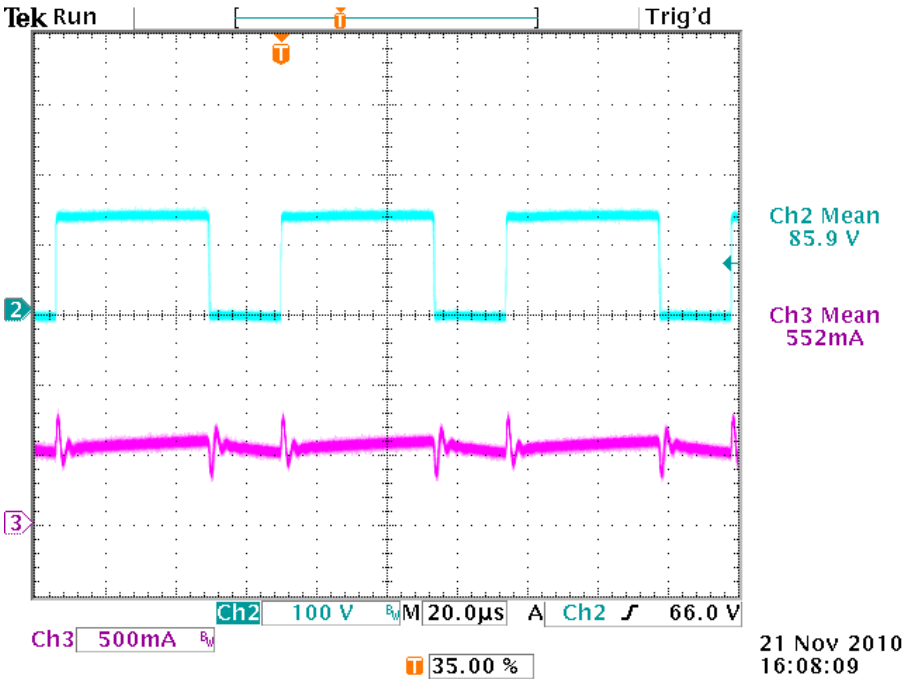

Armature voltage and current at 4 lbf-in commanded and 1500 rpm

In summary, separate-winding excitation DC motor operational theory was validated. A program was then written to output user defined, torque from the DC motor. The double-fed induction generator control system or any other research requiring a DC motor with commanded torque now has a controlled means of operation for further research opportunities.

THIS PAGE INTENTIONALLY LEFT BLANK

LIST OF ACRONYMS AND ABBREVIATIONS

A	Amperes
DC	Direct Current
DFIG	Doubly Fed Induction Generator
FPGA	Field Programmable Gate Array
GUI	Graphic User Interface
H	Henries
L	Inductance
L_{AF}	Mutual Armature and Field Inductance
PI	Proportional Integrator
SDC	Student Design Center
V	Volts
V_{DC}	DC Link Voltage

THIS PAGE INTENTIONALLY LEFT BLANK

ACKNOWLEDGMENTS

I would like to thank the faculty and staff at the Naval Postgraduate School for their outstanding support while attaining a higher level of education. I particularly want to point out my gratitude to my thesis advisor, Professor Alex Julian, for his guidance and support through the completion of this thesis. Without your knowledge and time spent guiding me, I would not have completed this thesis in the time allowed.

Most importantly, I would like to thank my beautiful and patient wife, Keri, and my kids, Sammantha and Jacob, for supporting me through this very time-consuming process of completing this thesis. Your love and patience have given me this great opportunity to succeed in my professional career.

THIS PAGE INTENTIONALLY LEFT BLANK

I. INTRODUCTION

A. BACKGROUND

U.S. Federal Agencies have been ordered by the President, and directed by law, to increase their use of renewable energy sources. The Energy Policy Act of 2005 requires by the year 2013 that 7.5 percent of electrical energy used by federal agencies come from renewable energy sources. This goal must increase to 25 percent total facility energy consumption by the year 2025 [1]. With the move towards renewable and recyclable energy creation, it becomes apparently clear that shifting energy consumption on federal installations towards non-fossil fuel technology is needed.

Wind technology is increasing growing and reliable source of renewable energy consumption. According to the American Wind Energy Association, the installed capacity of wind grew at an average of twenty-nine percent per year from 2002-2007 [2]. Harnessing this technology for use on federal installations and improving the efficiency of the system would add to the goal of reducing fossil fuel energy consumption on federal installations.

In December 2009, the Naval Postgraduate School finished developing a laboratory doubly-fed induction generator (DFIG) control system [3]. The DFIG control system is designed to provide stable electric power from wind turbines. A DFIG system is shown in Figure 1 [4].

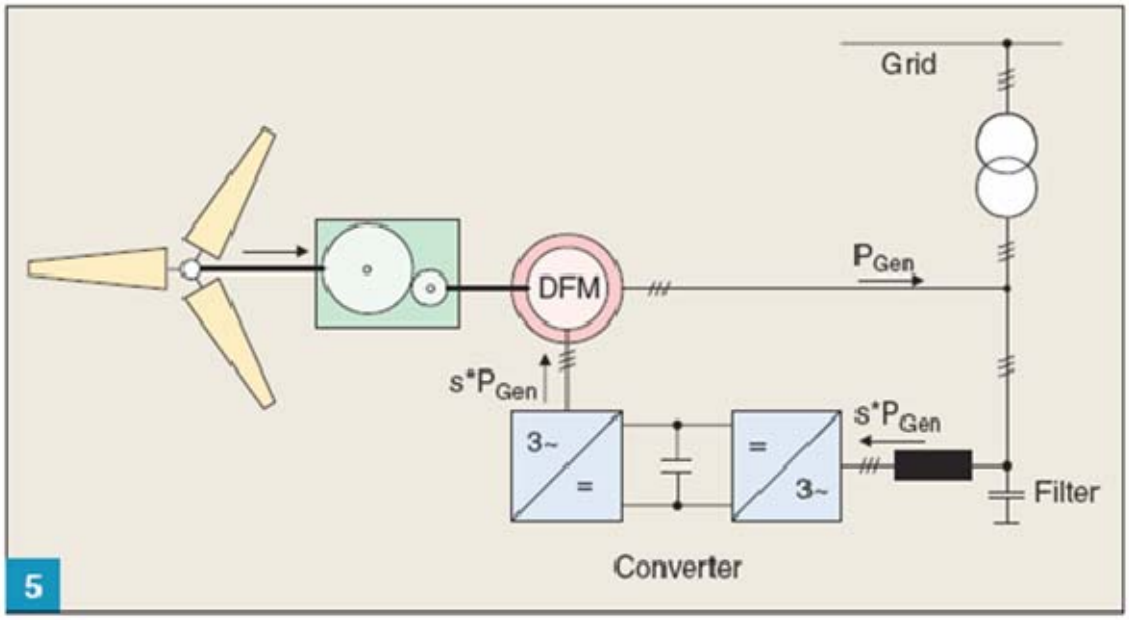

Figure 1. Doubly-fed induction generator wind turbine system, from [4].

To simulate wind speed and torque provided to the DFIG, the DFIG is mechanically pushed by a direct current (DC) motor shown in Figure 2.

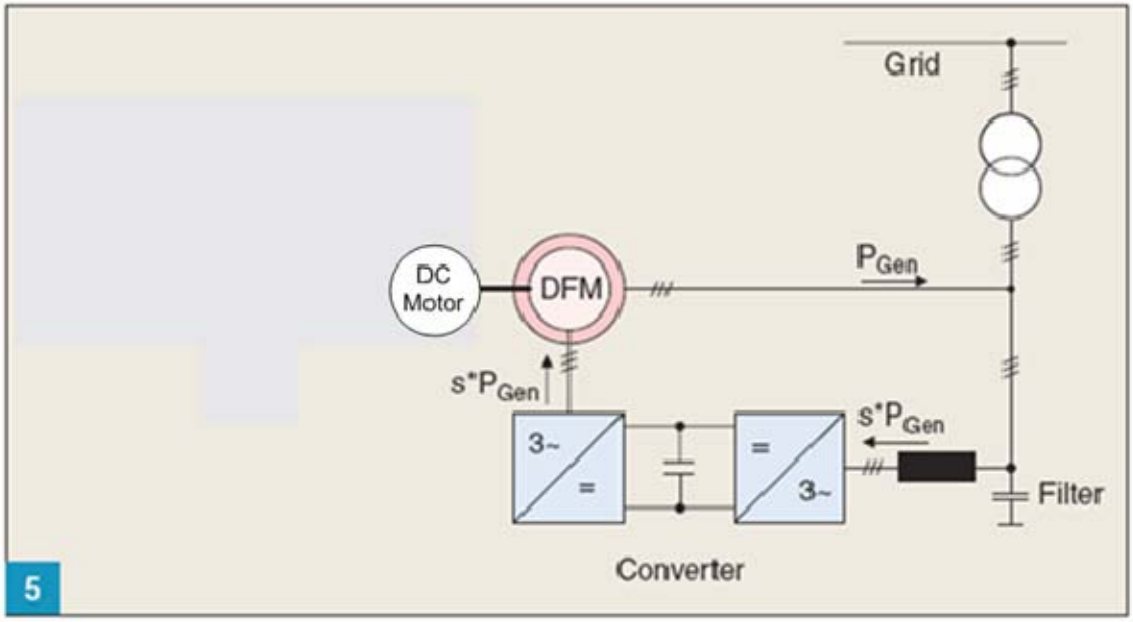

Figure 2. Doubly-fed induction generator wind turbine system modified, from [4].

Use of a DC motor [3] is a cheap and efficient way to provide torque and speed to the system for lab testing. However, the torque provided by the DC motor used in [3] is unmeasured and undetermined as to how much torque is being provided to the DFIG system.

B. OBJECTIVE

The purpose of the thesis was to have a better understanding how DC machines operate in order to choose the correct setup to provide the best output torque. The setup chosen should be easily predictable on performance for easier control. After choosing the best DC motor setup for torque and predictability, we wrote a user-friendly program to command accurate and sustained output torque to a DC motor.

C. APPROACH

The approach of this thesis was based on analysis of separate-winding excitation setup of a DC motor. Following validation of the theory, we wrote a computer program to allow a user to command how much electric torque the DC motor will output. First, a basic understanding of the theory of DC motor operation and behavior of separate-winding excitation setup is required before programming can be developed. The DC motor theory was researched from [5], [6], and [7]. Next, the components, equipment, and software were selected. Most of the equipment that was required were the same as used in [3], with the exception of an electro-dynamometer that was used in place of an induction generator to provide offsetting electric loads and the ability to measure output torque. Finally, a program was written based on DC machine theory using Matlab/Simulink and Xilinx software to program a Field Programmable Gate Array (FPGA) to control voltage or current to the motor. A Graphic User Interface (GUI) was used to order up desired output torque of the DC motor.

D. THESIS ORGANIZATION

This thesis is organized with the theory of separate-winding excitation DC motors, including the equations that represent torque, rotor speed, field and armature currents and voltages, covered in Chapter II. These values are profiled for the Labvolt DC motor used for testing.

Two computer simulation models were written in Simulink and are detailed in Chapter III. Test setup and results for each test is presented and performance is explained in detail.

Results of the testing and conclusions about the DC motor performance are addressed in Chapter IV. Recommendations on future work are suggested for additional research regarding DC motor commanded torque.

Date sheets for equipment used, Matlab code, Simulink models, a hexadecimal conversion datasheet for desired torque output on the Graphical User Interface (GUI) are detailed in the Appendixes.

II. DC MACHINE THEORY

A. INTRODUCTION

In this chapter, the theory of DC motor operations is reviewed from reference [5]. The theory is then validated by testing the setup of a 120-volt DC motor to validate the theory. Finally, the results of the Labvolt DC motor operations test are documented for future research opportunities.

B. DC MOTOR THEORY

1. Overview

There are multiple ways to operate a DC machine, either as a motor or a generator. For this thesis, a motor operation is selected because our main objective is to control output torque of a DC motor to drive a DFIG [3]. A DC motor can be set up in multiple ways. Four different, ways to control torque are described in [5]: Separate-Winding Excitation, Shunt-Connected, Series-Connected, and Compound-Connected.

Separate-Winding Excitation is a simple setup where the circuit is separated into two separate circuits. One side is a field circuit that is used to produce a field flux and the other side is an armature circuit that provides current to the rotor via brush and commutator. The interaction of the field flux and armature current in the rotor produces torque. The remainder of this thesis will focus on Separate-Winding Excitation, which will be explained in more detail later on.

A Shunt-Connected DC motor uses the same theory as Separate-Winding Excitation with the exception that the two circuits are connected in parallel instead of having separate voltage sources. By connecting the circuits in parallel, the field voltage is equal to the armature voltage. A Shunt-Connected DC motor is the most common industry setup because the motor will run at constant speed regardless of load. Its disadvantage is the torque potential of the motor will drop as more load is placed on the motor. A field rheostat is commonly used to adjust the field current to control the rotor

speed of the DC motor. Example uses of a Shunt-Connected DC Motor are machine lathes and manufacturing lines where speed and tension control are more important.

A Series-Connected DC motor still uses a field and an armature circuit like the Separate-Winding Excitation and Shunt-Connected DC Motor except the field circuit is connected in series with the armature circuit. Connecting the field and armature circuit in series causes the field current to equal the armature current. This set up allows the motor speed to adjust with torque load. The advantage to Series-Connected DC Motors is higher start-up torque. Its disadvantage is that in only allows operation for short periods of time and not continuous operation. Examples of uses for series-connected DC motors include crane hoists where heavy load will be raised or traction motors used to drive trains to get massive amounts of weight moving or an automobile starter motor.

A Compound-Connected DC Motor uses a combination of both Shunt and Series-Connected to combine the characteristics of both. The Compound-Connected DC Motor has to two field circuits and one armature circuit. One of the field circuits is connected in parallel with the armature circuit, and the other field circuit is connected in series with the armature circuit. The advantage to a Compound-Connected motor is that the motor will keep constant speed regardless of load changes like the Shunt-Connected DC motor and will respond better to higher torque demands like the Series-Connected DC motor. Some common uses of Compound-Connected DC motors include elevators, air compressors, and conveyors.

2. DC Motor Basic Concept and Equations

To understand how to control or command output torque of a DC motor, a review some of the basics of dc machine operations was looked at to understand the relationship of electric torque to the field and armature voltages and currents.

An elementary 2-pole DC machine is shown in Figure 3 [5]. The DC machine is equipped with a field winding wound on the stator poles, a rotor coil (a-a') and a commutator. A commutator is a usually made up of two semi-circular copper segments mounted on the shaft at the end of the rotor and insulated from each other. The terminals

of the rotor coils are connected to a copper segment. Stationary carbon brushes ride upon the copper segments so that the rotor coil is connected to a stationary circuit by a nearby frictionless contract [5].

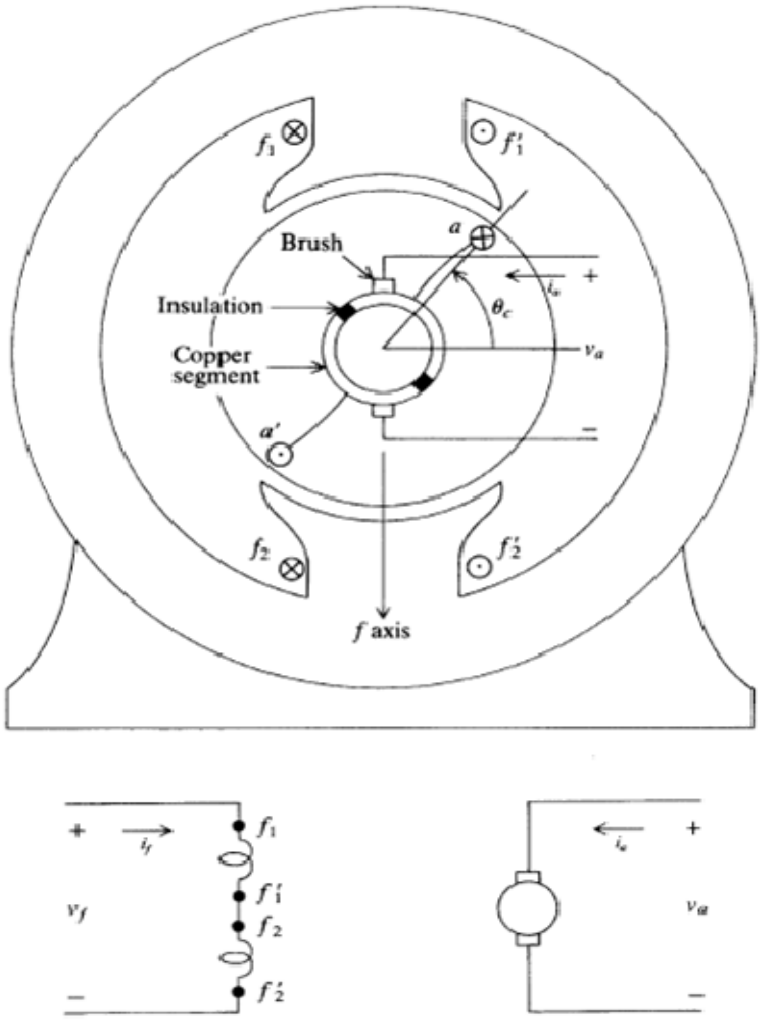

Figure 3. Elementary 2-pole DC machine, from [5].

The armature coils rotate in a magnetic field established by current flowing in the field winding. Voltage is induced in these coils by this rotation. The action of the commutator causes the armature coils to appear as a stationary winding with its axis orthogonal to the magnetic axis of the field winding. As a result, voltages are not induced in one winding due to the time rate of change of the current flowing in the other [4].

These conditions, derived from [5], define the field voltage $\left(v_f\right)$ and armature voltage $\left(v_a\right)$ in matrix form as

$$\begin{bmatrix} v_f \\ v_a \end{bmatrix} = \begin{bmatrix} r_f + \dfrac{d}{dt}L_{FF} & 0 \\ \omega_r L_{AF} & r_a + \dfrac{d}{dt}L_{AA} \end{bmatrix} \begin{bmatrix} i_f \\ i_a \end{bmatrix}, \tag{2.1}$$

where i_f and i_a are the field and armature currents, r_a and r_f are the armature and field resistance, and L_{AA} and L_{FF} are the self-inductance of the armature and field windings, respectively. L_{AF} is the mutual inductance between the armature and field windings, and ω_r is the rotor speed.

An equivalent circuit of a DC machine, shown in Figure 4, defines where these variables are identified. On the right side of Figure 4, or the armature circuit side, the voltage induced from the motor action is equal to $L_{AF}\omega_r i_f$. This is sometimes referred to as the back emf. $L_{AF}\omega_r i_f$ also represents the open-circuit armature voltage $\left(v_a\right)$ [5].

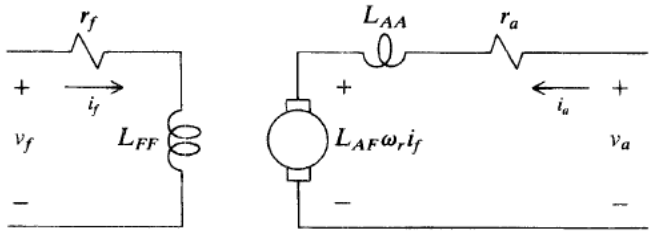

Figure 4. Equivalent circuit of a dc machine, from [5].

From [5], electric torque T_e is defined by its mutual inductance and the field and armature current as

$$T_e = L_{AF} i_f i_a . \tag{2.2}$$

Electric torque is equivalent to mechanical torque and is defined in [5] as

$$T_e = J\frac{d\omega_r}{dt} + B_m\omega_r + T_L \quad , \tag{2.3}$$

where J is the inertia of the rotor, B_m is the damping coefficient, T_L is the load torque that opposes the electric torque.

3. Separate-Winding Excitation DC Motor Equations

Separate-winding excitation is a basic DC motor setup that is similar to Figure 4 with the exception of a variable field rheostat is added to the circuit. A field rheostat is used to adjust the field current in the circuit. In Figure 5, an equivalent circuit, similar to Figure 4, with a field rheostat is shown. Reference [5] defines the rheostat as r_{fx}.

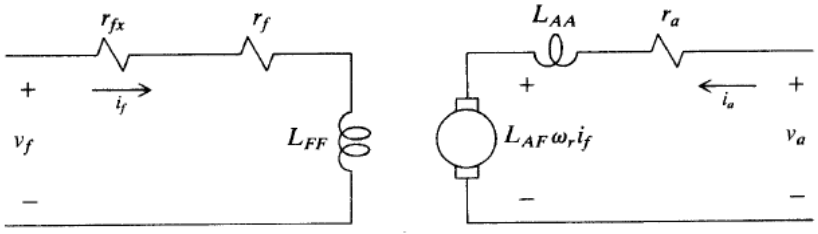

Figure 5. Equivalent circuit for separate field and armature excitation, from [5].

When the DC motor is at steady state, [4] defines the field voltage as

$$V_f = R_f I_f \, . \tag{2.4}$$

The total field resistance R_f is equal to the field rheostat value r_{fx} plus the field circuit resistance r_f. The capital letter denotes steady state values for current and voltage [4].

The armature voltage at steady-state operation is [5]

$$V_a = r_a I_a + \omega_r L_{AF} I_f \, . \tag{2.5}$$

Rearranging Equation (2.5) to solve for I_a, we get

$$I_a = \frac{V_a - \omega_r L_{AF} I_f}{r_a}. \tag{2.6}$$

Substituting Equation (2.6) into (2.2), we get

$$T_e = L_{AF} I_f \left(\frac{V_a - \omega_r L_{AF} I_f}{r_a} \right). \tag{2.7}$$

The mutual inductance L_{AF} has a constant value. If the field voltage V_f and total field resistance R_f are held to a constant value, I_f will stay constant. Therefore, reference [5] introduces a new variable k_v to simplify the product of these constants as

$$k_v = L_{AF} I_f. \tag{2.8}$$

Therefore, to simplify Equation (2.7) further, we substitute (2.8) into (2.7) to get

$$T_e = k_v \left(\frac{V_a - \omega_r k_v}{r_a} \right). \tag{2.9}$$

From Equation 2.9, we can now predict the electric torque T_e at a given speed ω_r if the armature voltage V_a is constant at steady-state conditions. Inversely, we can also predict ω_r at a given T_e for a constant V_a.

C. EQUIPMENT SETUP FOR PERFORMANCE TESTING OF THEORY

Some of the components used in this experiment were the same that were used in [3] for the purpose of follow-on work compatibility with [3]. The equipment used for this experiment and shown in Figure 6 and detailed in Appendix A: Student Design Center (SDC) – Reference [8], Semi-stack IGBT, AC/DC Power Supply, 175W DC motor, Electrodynamometer, Tachometer, Computer with Matlab/Simulink and Xilinx Software, and Oscilloscope and Multimeters.

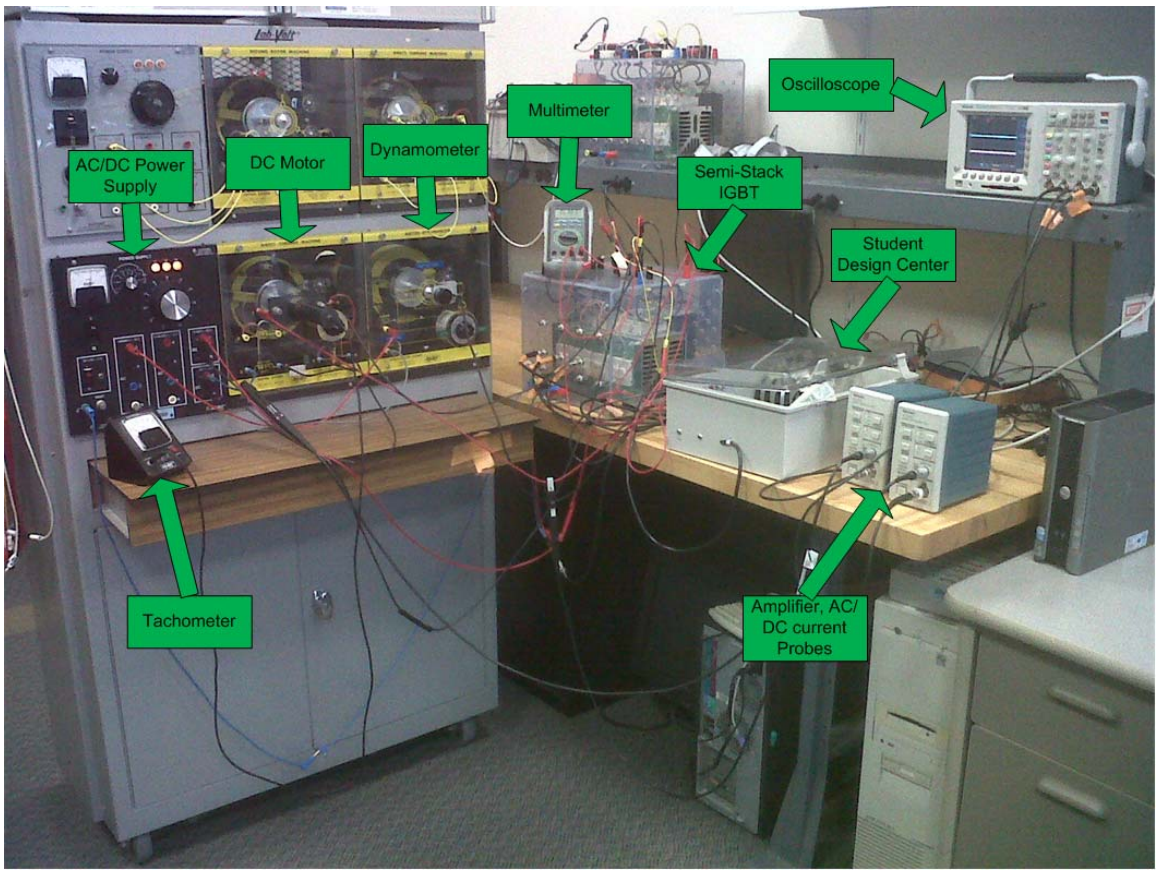

Figure 6. Photograph of equipment used.

In Figure 7, a schematic diagram of the equipment setup for this experiment is shown.

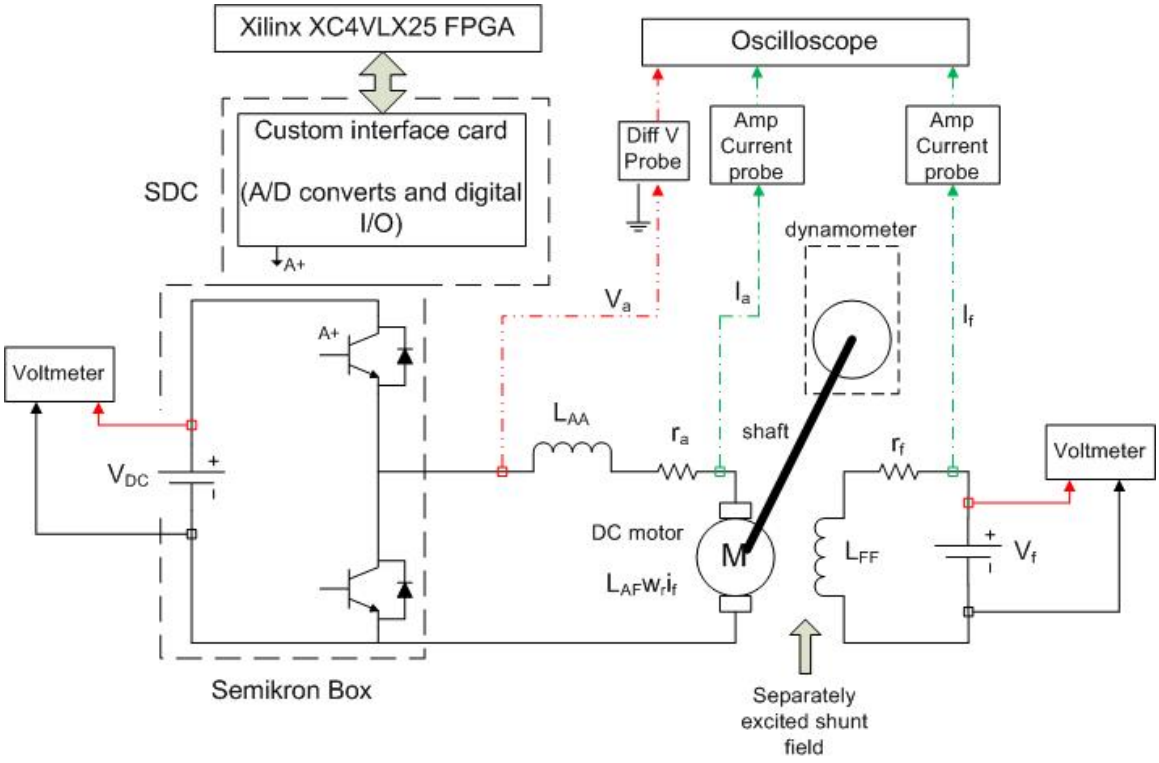

Figure 7. Equipment Setup Schematic.

From the AC/DC power supply, the 120 V_{DC} constant source, node 8, was used on the field side of the DC motor since a constant field voltage is desired. The field voltage measured 132 V but stayed constant with each test.

The armature voltage required also needed to be constant, but the variable source in the range 0-120 V_{DC} was used on the armature side so that the armature voltage could be changed between tests. The variable voltage power supply connected with the supply side of the Semistack-IGBT.

The Semistack-IGBT, manufactured by SEMIKRON and shown in Appendix A, was used to manipulate space vector manipulation (SVM) in [3]. Though SVM is not required for this thesis directly, the design utilizes an available port on the DFIG side SEMISTACK-IGBT of [3].

A square wave generator program, shown in Figures 8 and 9, was written in Matlab/Simulink with Xilinx software to provide a better constant armature voltage than that supplied directly from the AC/DC power supply. This program was written utilizing the same Chipscope Interface, Data Conversion, and A-to-D conversion, and encoder blocks of [3].

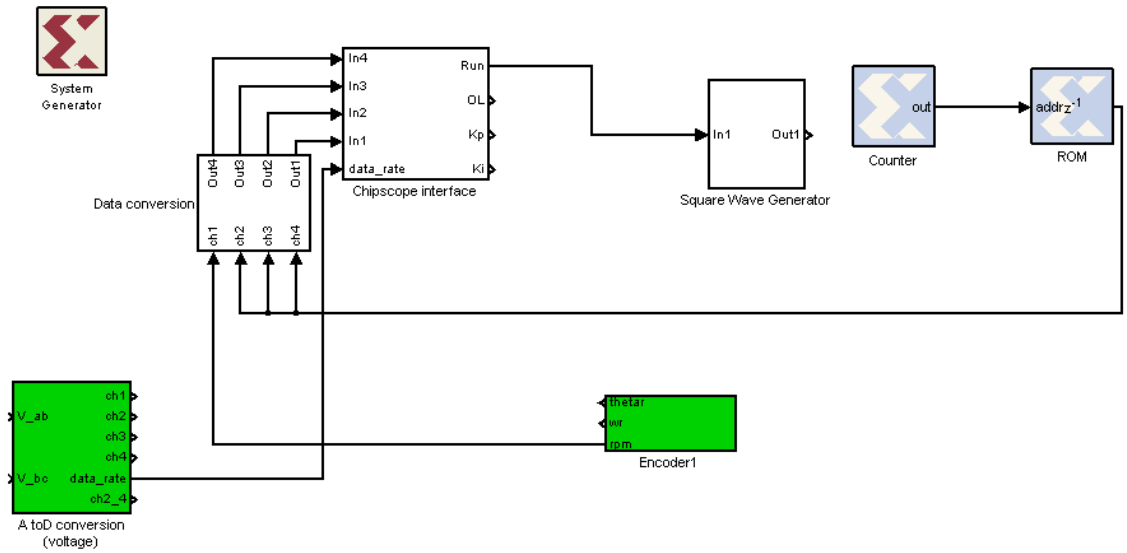

Figure 8. Matlab/Simulink Program for constant armature voltage.

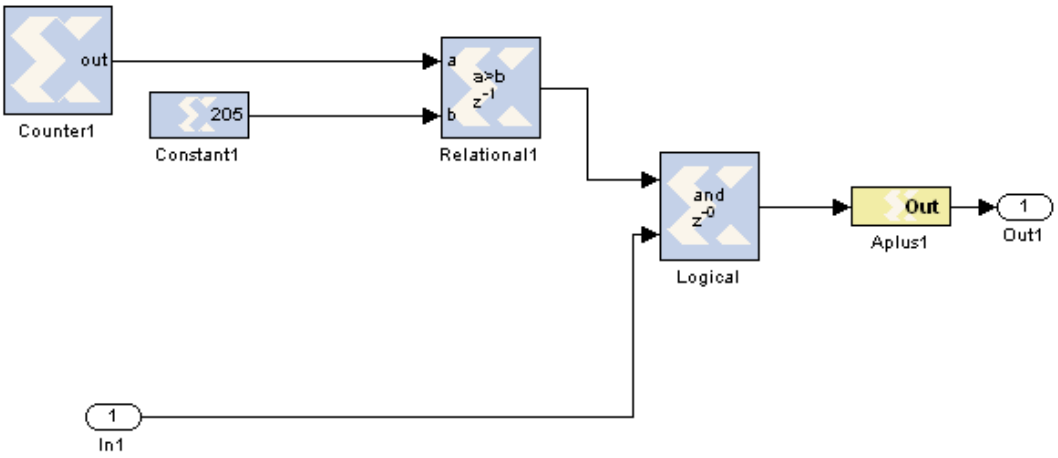

Figure 9. Square Wave Generator block from Figure 8.

An electro-dynamometer, shown in Appendix A, was used to provide a load to the DC motor. At steady-state conditions, the load torque T_L is equal to the electric torque T_e [5]. The load torque was increased or decreased on the dynamometer by adjusting the amount of AC current supplied to the dynamometer. The dynamometer measured load torque in pound-force-inches (lbf-in).

Measurements of torque and speed were taken at three different armature voltages to profile and measure the Labvolt, DC motor. These measurements will also help to identify the values of k_v, r_a, L_{AF}, R_f, which are not listed on the specifications sheet in Appendix A.

D. RESULTS

In this section, the Separate-Winding Excitation DC motor theory is validated. The results of the following tests can be used to profile the Labvolt DC machine for future research. Tests were completed at three different supplied armature voltages and graphed to profile the torque versus speed profile.

1. Initial Values and Measurements

The Labvolt DC motor, shown in Appendix A, is rated at ¼ shaft horsepower, 120 V, 2.8 A, and 1800 rpm. The armature and field resistances were measure using a mulitmeter.

The armature resistance r_a measured to be 8.5 Ω using a multimeter. The armature resistance was measured across the armature terminals with the brushes of the rotor in series with the field windings.

The field resistance R_f was measured after the initial armature voltage was set for the first test. An initial armature voltage of 110 V was selected by adjusting the variable DC voltage power supply until the average voltage across the motor measured 110 V on an oscilloscope. No load torque was applied on the dynamometer. The rheostat was then adjusted on the field circuit so that the initial test speed was measured to be 1800 rpm on the tachometer. The field resistance R_f, which is the field resistance

plus the applied rheostat resistance, measured to be 644 Ω using a multimeter. The field resistance was measured across the field windings in series with the adjusted rheostat. For the remainder of the test, the rheostat was locked in place and never adjusted so that R_f remained constant throughout all tests.

The DC machine inductance values were also not initially known. The mutual inductance is the only measurement needed in order to calculate torque. The mutual inductance was calculated using power Equations from [6] and [9]. Power out is calculated as the product of the torque and rotor speed, which is equivalent to the products of the armature and field currents and voltages supplied minus power losses. Equating these two powers, we get

$$P_{out} = T_e \omega_r = V_a I_a + V_f I_f - P_{loss}. \tag{2.10}$$

Power losses are estimated by the products of the armature and field resistances and currents squared, neglecting friction, windage, and core losses on the basis that they are minimal. Power loss is approximately calculated from

$$P_{loss} \simeq I_a^2 r_a + I_f^2 r_f. \tag{2.11}$$

Now substituting (2.11) into (2.10) and solving for T_e, we get

$$T_e = \frac{V_a \cdot I_a + V_f \cdot I_f - \left(I_a^2 \cdot r_a + I_f^2 \cdot r_f \right)}{\omega_r}. \tag{2.12}$$

The initial values, which are measured on an oscilloscope, multimeter, and tachometer to determine initial torque, are tabulated in Table 1.

Table 1. Initial measurements.

Initial Measurements	
V_a	110 V
V_f	132 V
I_a	0.38 A
I_f	0.20 A
ω_r	1800 rpm = 188.5 rad/s
r_a	8.5 Ω
R_f	644 Ω

Using Equation (2.12) and the initial values measured, we initially calculated

$$T_e = \frac{(110V)(0.38A)+(132V)(0.20A)-\left((0.38A)^2(8.5\Omega)+(0.20A)^2(644\Omega)\right)}{188.5rad/s}$$
$$T_e = 0.219N\cdot m \quad .(2.13)$$

The mutual inductance was then calculated by rearranging Equation (2.2) to obtain

$$L_{AF} = \frac{T_e}{i_f \cdot i_a} . \quad (2.14)$$

From Equation (2.14), the mutual inductance L_{AF} at the initial test was calculated as

$$L_{AF} = \frac{0.219N\cdot m}{(0.38A)(0.20A)} = 2.88H . \quad (2.15)$$

From Equation (2.8), the constant k_v was calculated as

$$k_v = (2.88H)(0.20A) = 0.576A\cdot H . \quad (2.16)$$

2. Measured Values at Set Armature Voltages

The measured values at different torque loads, the calculated mutual inductance L_{AF} using Equation (2.14), and the calculated electric torque using Equation (2.7) at set armature voltages of 110 V, 121 V and 100 V are shown in Tables 2 through 4. The calculated torque tabulated in Tables 2 through 4 was calculated using Equation (2.12) in units of Newton-meters. The torque conversion factor to convert units of Newton-meters to pound-force-inches is $0.11298 \, {lbf \cdot in}/{N \cdot m}$. The calculated mutual inductance listed in Tables 2 through 4 was calculated using Equation (2.14). The torque value for the calculated mutual inductance used the torque calculated by Equation (2.12) in Newton-meters and the measured field and armature current.

Table 2. Measured values and calculated T_e and L_{AF} at V_a = 110 V.

Measured						Calculated		
$T_L\,(lbf \cdot in)$	$V_f\,(V)$	$I_f\,(A)$	$V_a\,(V)$	$I_a\,(A)$	$\omega_r\,(rpm)$	$L_{AF}\,(H)$	$T_e\,(N \cdot m)$	$T_e\,(lbf \cdot in)$
0	132	0.20	110	0.38	1800	2.88	0.22	1.94
1	132	0.20	110	0.57	1750	2.90	0.33	2.93
2	132	0.20	110	0.77	1700	2.93	0.45	4.00
3	132	0.20	110	0.93	1650	2.98	0.55	4.90
4	132	0.20	110	1.1	1600	3.02	0.67	5.89
5	132	0.20	110	1.3	1575	3.02	0.78	6.94
6	132	0.20	110	1.5	1550	3.01	0.90	7.99
7	132	0.20	110	1.8	1500	3.03	1.09	9.64
8	132	0.20	110	2.0	1475	3.02	1.21	10.70
9	132	0.20	110	2.2	1450	3.02	1.33	11.75
10	132	0.20	110	2.4	1400	3.07	1.47	13.02
11	132	0.20	110	2.7	1375	3.03	1.64	14.49
12	132	0.20	110	2.9	1350	3.03	1.76	15.54
13	132	0.20	110	3.2	1325	2.99	1.91	16.94
14	132	0.20	110	3.4	1300	2.99	2.03	17.97
15	132	0.20	110	3.8	1275	2.92	2.22	19.62
16	132	0.20	110	4.0	1250	2.91	2.33	20.60

Table 3. Measured values and calculated T_e and L_{AF} at V_a = 121 V.

Measured						Calculated		
$T_L\,(lbf \cdot in)$	$V_f\,(V)$	$I_f\,(A)$	$V_a\,(V)$	$I_a\,(A)$	$\omega_r\,(rpm)$	$L_{AF}\,(H)$	$T_e\,(N \cdot m)$	$T_e\,(lbf \cdot in)$
0	132	0.2	121	0.38	2000	2.86	0.22	1.92
1	132	0.2	121	0.58	1925	2.91	0.34	2.99
2	132	0.2	121	0.75	1875	2.95	0.44	3.91
3	132	0.2	121	0.9	1800	3.03	0.55	4.83
4	132	0.2	121	1.1	1750	3.07	0.67	5.97
5	132	0.2	121	1.3	1725	3.06	0.80	7.04
6	132	0.2	121	1.5	1675	3.10	0.93	8.23
7	132	0.2	121	1.8	1650	3.07	1.11	9.78
8	132	0.2	121	2	1600	3.12	1.25	11.03
9	132	0.2	121	2.1	1575	3.14	1.32	11.66
10	132	0.2	121	2.4	1550	3.11	1.49	13.21
11	132	0.2	121	2.6	1525	3.11	1.62	14.29
12	132	0.2	121	2.8	1500	3.10	1.74	15.38
13	132	0.2	121	3.1	1450	3.12	1.94	17.15
14	132	0.2	121	3.3	1425	3.12	2.06	18.24
15	132	0.2	121	3.7	1400	3.06	2.27	20.05
16	132	0.2	121	4	1375	3.03	2.42	21.44

Table 4. Measured values and calculated T_e and L_{AF} at V_a = 100 V.

Measured						Calculated		
$T_L\,(lbf\cdot in)$	$V_f\,(V)$	$I_f\,(A)$	$V_a\,(V)$	$I_a\,(A)$	$\omega_r\,(rpm)$	$L_{AF}\,(H)$	$T_e\,(N\cdot m)$	$T_e\,(lbf\cdot in)$
0	133.1	0.2	100	0.5	1625	2.86	0.29	2.53
1	133.1	0.2	100	0.6	1575	2.92	0.35	3.10
2	133.1	0.2	100	0.8	1525	2.95	0.47	4.18
3	133.1	0.2	100	0.9	1500	2.97	0.53	4.73
4	133.1	0.2	100	1.1	1475	2.96	0.65	5.76
5	133.1	0.2	100	1.4	1425	2.97	0.83	7.37
6	133.1	0.2	100	1.6	1400	2.96	0.95	8.40
7	133.1	0.2	100	1.8	1375	2.96	1.06	9.42
8	133.1	0.2	100	2	1350	2.95	1.18	10.45
9	133.1	0.2	100	2.2	1325	2.94	1.30	11.46
10	133.1	0.2	100	2.4	1300	2.94	1.41	12.47
11	133.1	0.2	100	2.6	1250	2.99	1.55	13.75
12	133.1	0.2	100	2.8	1225	2.98	1.67	14.78
13	133.1	0.2	100	3.1	1175	3.00	1.86	16.48
14	133.1	0.2	100	3.4	1150	2.96	2.01	17.83
15	133.1	0.2	100	3.8	1125	2.88	2.19	19.39
16	133.1	0.2	100	4.1	1100	2.84	2.33	20.59

3. Results

From Tables 2 through 4, it was observed with each increase in load torque that the rotor speed decreased by 50 or 25 rpm. The calculated mutual inductance varied slightly and ranged from 2.84 to 3.14 H. The average mutual inductance was calculated to be 2.99 H. The standard deviation of the mutual inductance calculated to be 0.05, 0.09, and 0.07, respectively.

The calculated output torque was slightly higher than measured load torque in every measured point. This error is likely caused from the windage, friction and core losses discussed earlier. Other causes of error could be from the calibration accuracy of the dynamometer and the measurement of the armature current using an oscilloscope. Using a torque meter to measure torque would have been a better solution than relying on armature current and calculated mutual inductance for torque. However, no torque meter

was available at the time of testing, and it was assumed that load torque would be approximately equal to electric torque output for a separate-winding excitation DC motor from [4].

From the data tabulated in Tables 2 through 4, a plot of calculated electric torque versus measured rotor speed at the three different armature voltages is shown in Figure 10. At constant voltage, the calculated torque increases nearly linear as rotor speed decreases. For every unit of torque in pound force-inches, the rotor speed decreased 0.3 times the rotor speed in rpm. This was nearly linear because the calculated mutual inductance was nearly constant. At the three different armature voltage tested, the linear slope remained the same. The rotor speed was faster at higher armature voltage and no load torque. In conclusion, we have validated that torque is proportional to rotor speed at a constant armature voltage.

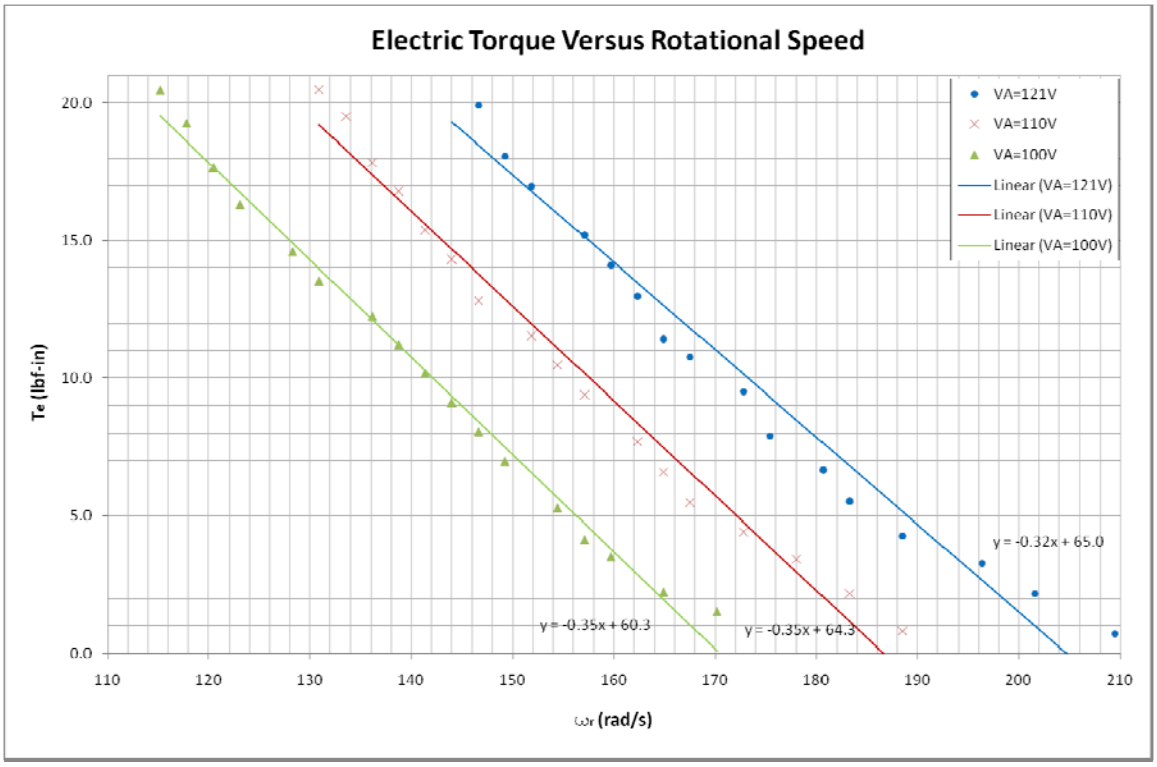

Figure 10. Electric torque versus rotor speed.

E. CHAPTER SUMMARY

The theory of separate-winding excitation DC motor operations was reviewed in this chapter. This theory was then validated in an experiment to find torque at a given speed and armature voltage. The experiment showed that the motor behaved predictably in the operating range in which it was tested. We will next take the theory validated in this chapter and use it to command the DC motor and output desired torque through Simulink Modeling with Xilinx embedded software.

THIS PAGE INTENTIONALLY LEFT BLANK

III. COMMANDING TORQUE

A. INTRODUCTION

Now that the torque can be predicted for a separate-winding excitation DC motor at a certain rotor speed, the motor can be programmed to output a torque from a user interface utilizing Matlab, Simulink, and Xilinx software. An attempt at commanded torque by controlling armature voltage is covered in this chapter. Finally, commanding torque by controlling armature current is covered.

B. COMMANDED TORQUE BY CONTROLLING ARMATURE VOLTAGE

1. Overview

A theory of controlling armature voltage for a given rotor speed and user-defined torque is covered in this section. This theory is then built into Simulink and tested on the separate-winding excitation DC motor through Xilinx software interface.

2. Controlling Armature Voltage Testing

A simulink program, which was written for an existing DC motor controls, the rotor speed for a separate-winding excitation DC motor [7]. In [7], armature voltage is the user-defined input to the DC motor, and rotor speed is measured.

We rewrote the program, which was written for [7], to require a user to input the desired torque vice the desired armature voltage. The DC motor is powered and controlled based on the user input.

In order to power the DC motor, the motor requires armature voltage. Rearranging Equation (2.9) to solve for armature voltage, we get

$$V_a = T_e\left(\frac{r_a}{k_v}\right) + \omega_r k_v . \tag{3.1}$$

the armature resistance r_a is still equal to 8.5 Ω as listed in Table 1. We selected the average mutual inductance to calculate k_v from Equation (2.8) as

$$k_v = L_{AF} I_f = (2.99H)(0.2A) = 0.6HA . \tag{3.2}$$

The rotor speed ω_r was measured through the encoder shown in Appendix A. The only variable remaining to satisfy Equation (3.1) is a user-defined torque required to output the needed armature voltage to drive the separate-winding excitation DC motor. The system needed to satisfy the desired output is shown in Figure 11.

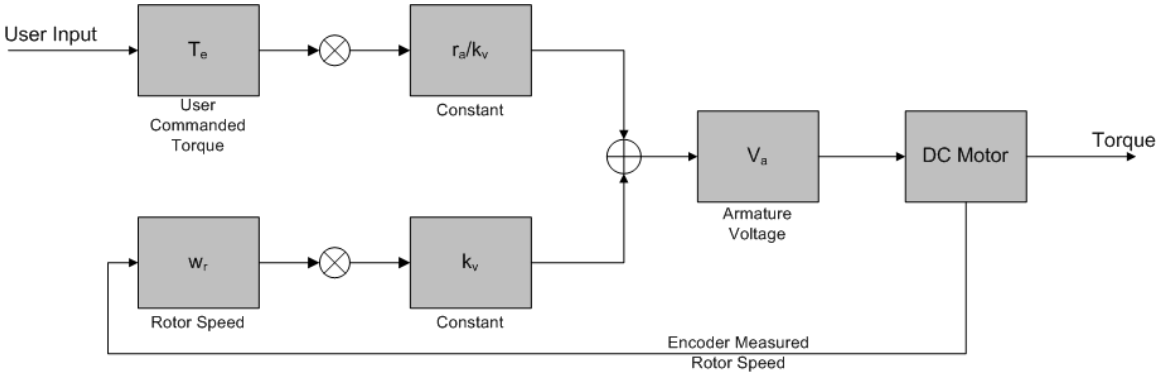

Figure 11. Commanding torque to output torque system diagram.

A Simulink program written to reflect the desired system shown from Figure 11 is shown in Figure 12.

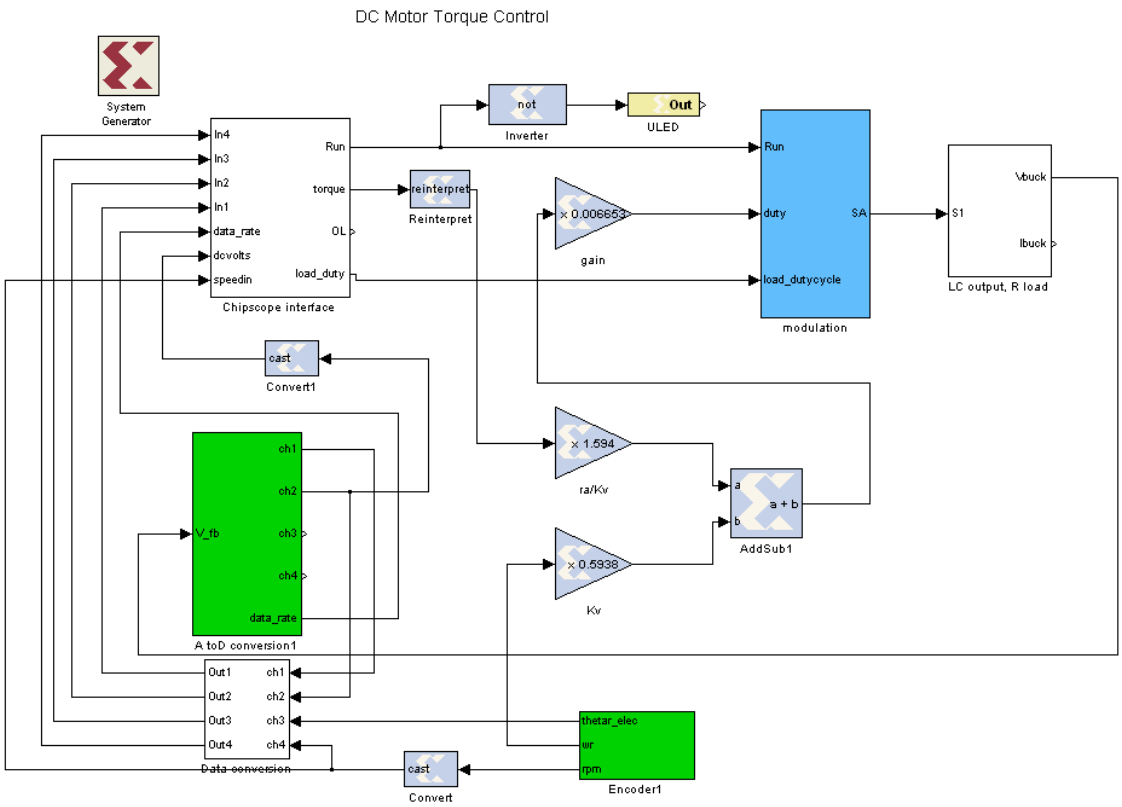

Figure 12. Simulink program for torque input and voltage controlled DC motor.

In Figure 12, the user-defined torque value goes from the torque node, on chipscope interface, to the product of r_a/k_v and is summed with the product of k_v and the measured rotor speed from the encoder. This voltage is sent through a gain and then modulated through a user defined duty cycle before being sent to the analog-to-digital signal block to be sent to the DC motor.

The equipment that was used and the setup were the same as in Chapter II from Figures 6 and 7. In Figure 13, the Xilinx Chipscope Pro Analyzer, Graphical User Interface (GUI) was used to active the DC motor and the user defined torque input. The torque input is in units of pounds-force inches, and the input units require a modified hexadecimal entry using the datasheet listed in Appendix D. Rotor speed measurement and DC voltage measurement from the power supply are also shown Figure 13 using regular hexadecimal values.

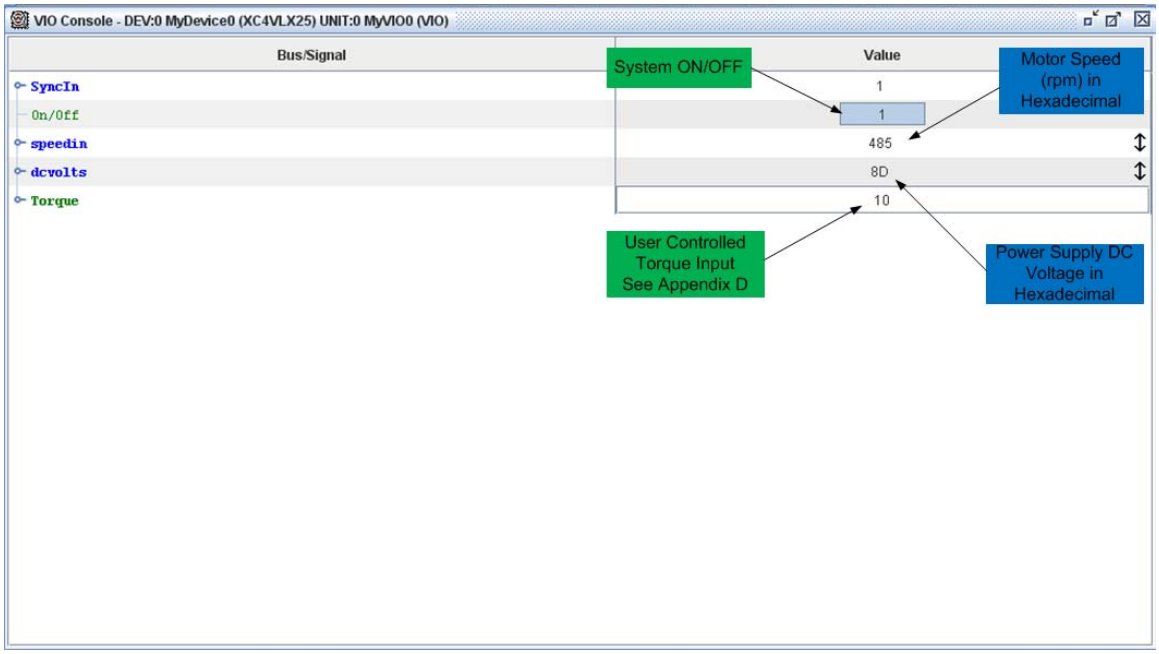

Figure 13. Xilinx chipscope pro analyzer graphical user interface.

3. Voltage Control of DC Motor Test Results

A torque meter was again not available so the output torque was calculated from Equation (2.2) using measured armature current i_a. Equation (3.1) was used to calculate armature voltage. The results for the commanded torque, voltage controlled test are shown in Table 5.

Table 5. Measured and calculated values for voltage control test.

Commanded	Measured				Calculated	
$T_e\,(lbf\cdot in)$	$T_L\,(lbf\cdot in)$	$\omega_r\,(rpm)$	$V_a\,(V)$	$I_a\,(A)$	$V_a\,(V)$	$T_e\,(lbf\cdot in)$
4	1.3	1500	93.2	0.574	100	3.05
4	1.6	1400	87.8	0.607	94.4	3.22
4	2.4	1000	63.6	0.792	69.2	4.20
8	2.8	1700	103	0.874	120	4.64
8	3.8	1400	85.3	1.02	101	5.41
12	5.5	1500	98.6	1.37	113	7.27
12	7	1300	80.5	1.71	101	9.08

4. Summary of Results

For this test, sustained output torque could not be achieved. From Table 5, it was observed again that adding load torque causes the rotor speed to decrease. As rotor speed was decreased, the armature voltage was decreased. As the armature voltage was decreased, the armature current was increased, and from the torque Equation (2.2), the output torque was increased. This is an unstable system since the calculated output torque can vary from load changes. For this system to work, constant rotor speed is required. The program does not account for load torque affecting rotor speed. In order for this system to work, the rotor speed has to be held steady. In the next section, commanding torque by closing the controlled loop of the armature current and not using measured rotor speed as a factor in applied power to the DC motor.

C. COMMANDED TORQUE BY CONTROLLING ARMATURE CURRENT

1. Overview

In this section, the torque of the separate-winding excitation DC motor is operated by controlling the armature current. This theory is then built into the Simulink program and tested on the DC motor.

2. Controlling Armature Current Testing

For this test, we used the theory discussed earlier in relation to Equation (2.2) to output desired torque by controlling the armature current though our Simulink Model.

Rearranging Equation (2.2) to solve for armature current, we get

$$i_a = \frac{T_e}{L_{AF} \cdot i_f} = \frac{T_e}{k_v}. \tag{3.3}$$

If the user-defined commanded torque was divided by the known constant k_v the output value is the armature current needed to operate the DC motor at the desired torque. The constant k_v used is the same as calculated for Equation (3.2). The armature current was controlled by a Proportional-Integral (PI) controller to modulate commanded current

with measured current to close the loop on the current to the DC motor. If the armature current is constant through any load and rotor changes, the output torque will remain constant.

The equipment that was used and the setup was the same as in Chapter II from Figures 6 and 7. The Simulink model from Figure 12 was altered to command torque by controlling the armature current as shown in Figure 14. The GUI that was used was the same as in the last section shown, in Figure 13, and used the same hexadecimal datasheet from Appendix D.

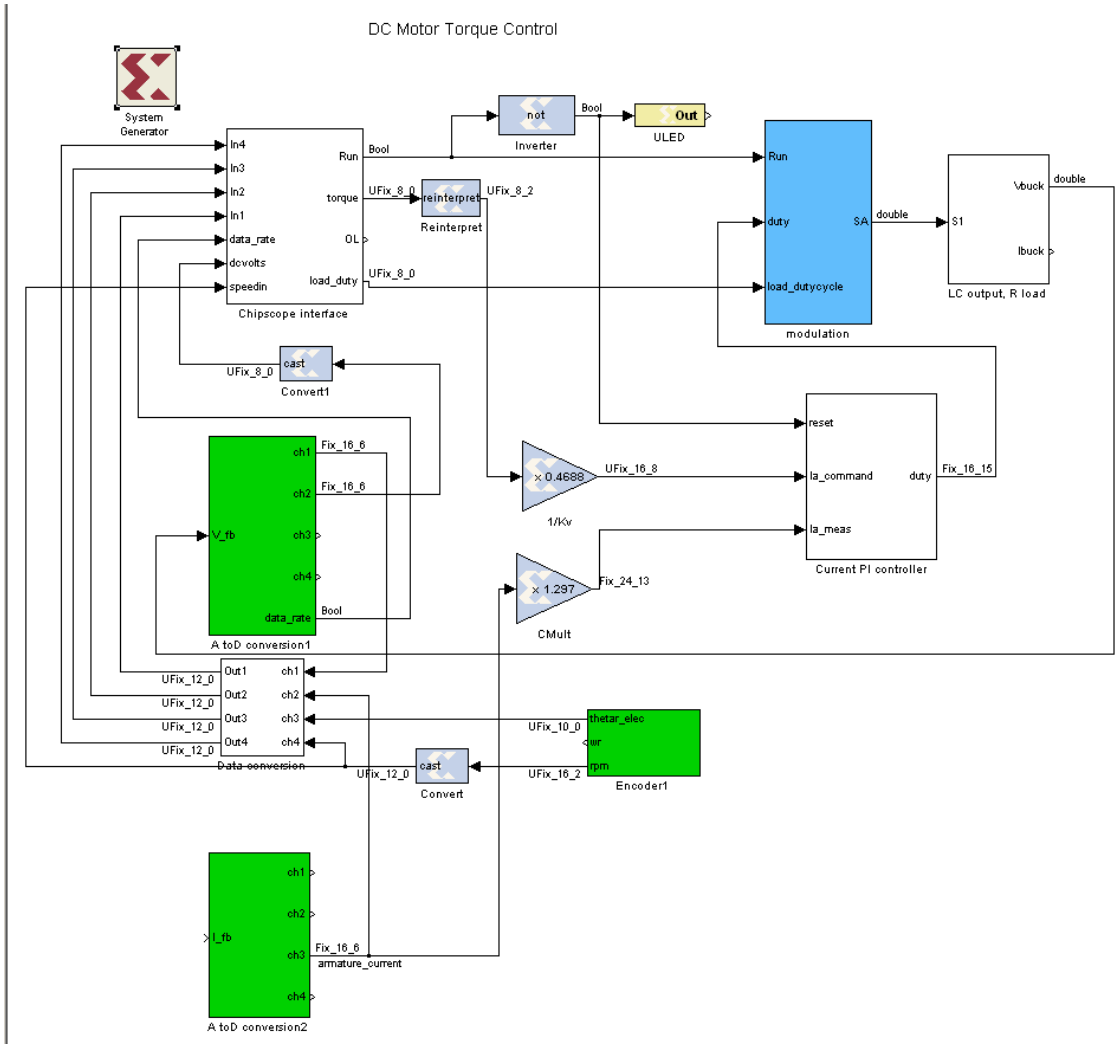

Figure 14. Simulink program for torque input and current controlled DC motor.

3. Current Control of DC Motor Test Results

The electro-dynamometer is still assumed as not a reliable way to measure output torque. Again with no torque meter available, the output torque was again calculated from Equation (2.2) using the measured armature current i_a. The results for commanding torque by controlling the armature current test are shown in Table 6.

Table 6. Measured and calculated values for current control test.

Commanded	Measured				Calculated	Notes
$T_e\,(lbf\cdot in)$	$T_L\,(lbf\cdot in)$	$\omega_r\,(rpm)$	$V_a\,(V)$	$I_a\,(A)$	$T_e\,(lbf\cdot in)$	
4	1.3	1900	110	0.55	2.92087	See Figure 15
4	1.6	1000	55.2	0.56	2.97398	
4	1.6	1500	85.9	0.55	2.92087	See Figure 16
8	6	1500	98.5	1.43	7.59426	See Figure 17
8	6	100	5.95	1.44	7.64737	
8	6	1300	82.1	1.41	7.48805	See Figure 18
8	6	1800	120	1.43	7.59426	
12	10.5	100	13.1	2.29	12.1614	
12	10	200	17.4	2.3	12.2146	

A few examples of oscilloscope measurements of the armature voltage and currents are shown in Figures 15–18. The top waveform in each figure shows the armature voltage, and the bottom waveform shows the armature current.

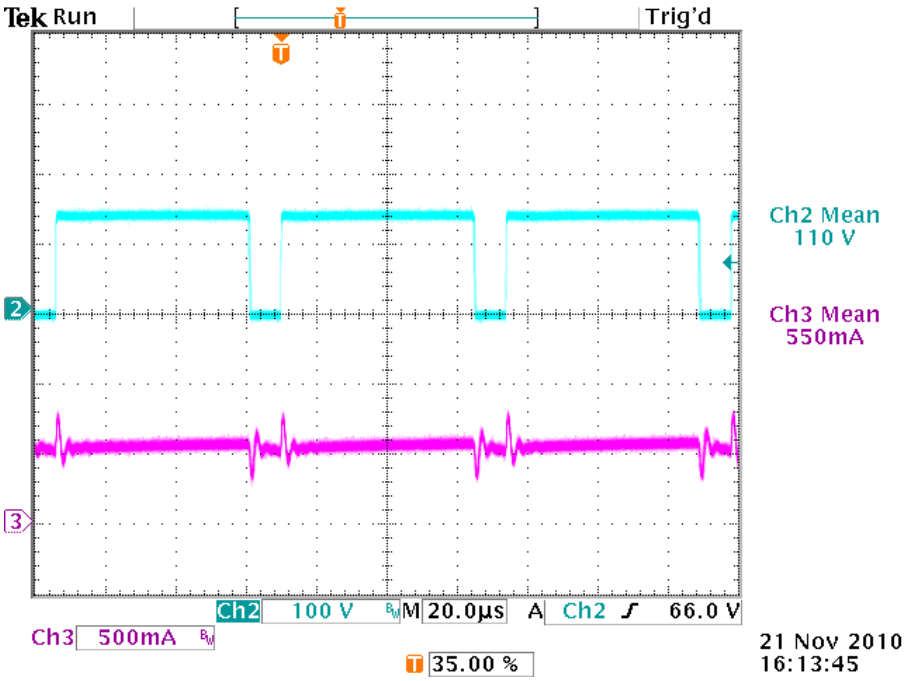

Figure 15. Armature voltage and current at 4 lbf-in commanded and 1900 rpm.

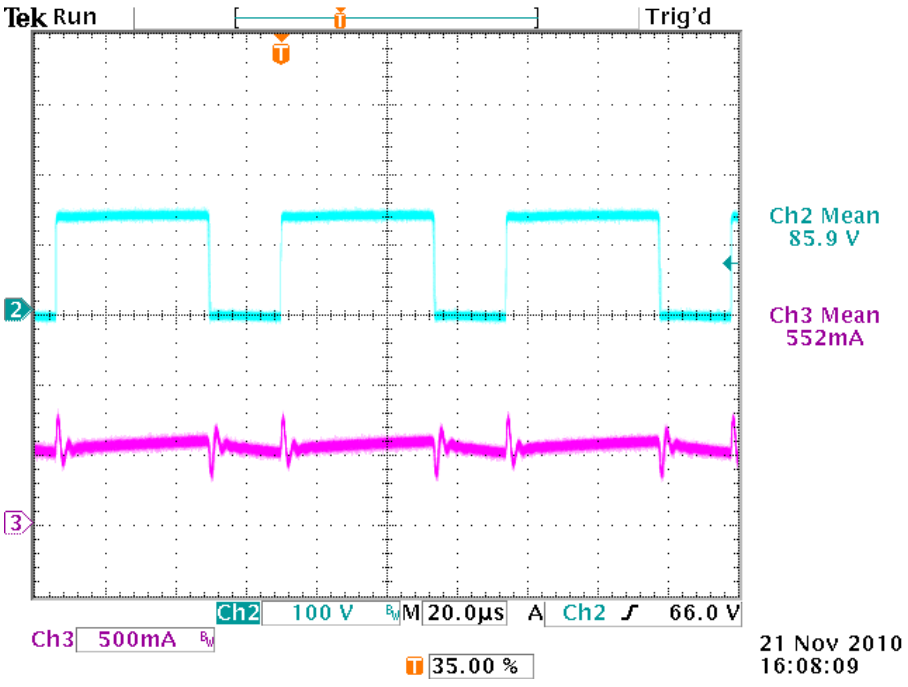

Figure 16. Armature voltage and current at 4 lbf-in commanded and 1500 rpm.

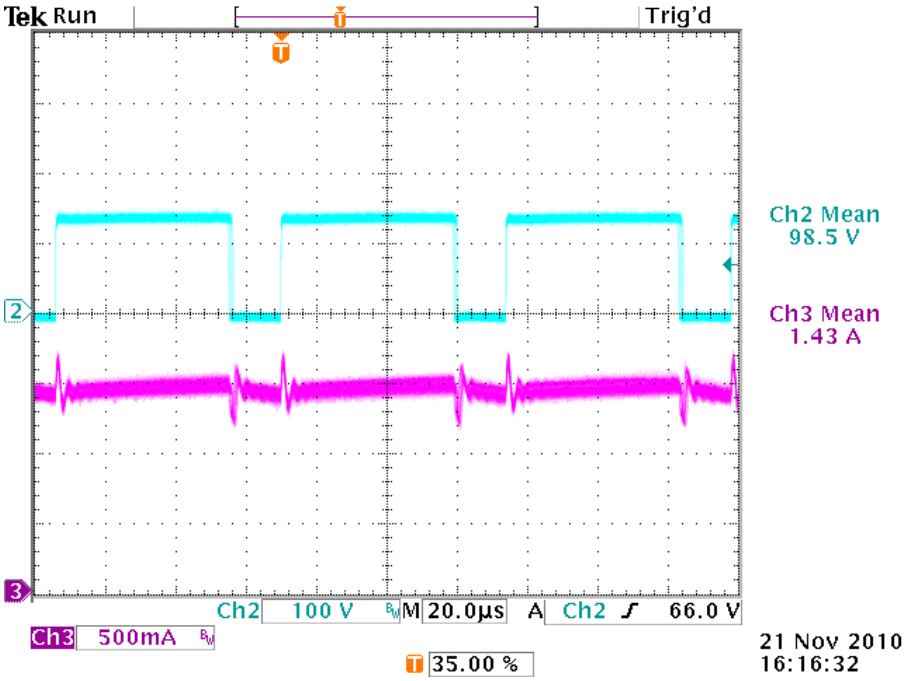

Figure 17. Armature voltage and current at 8 lbf-in commanded and 1500 rpm.

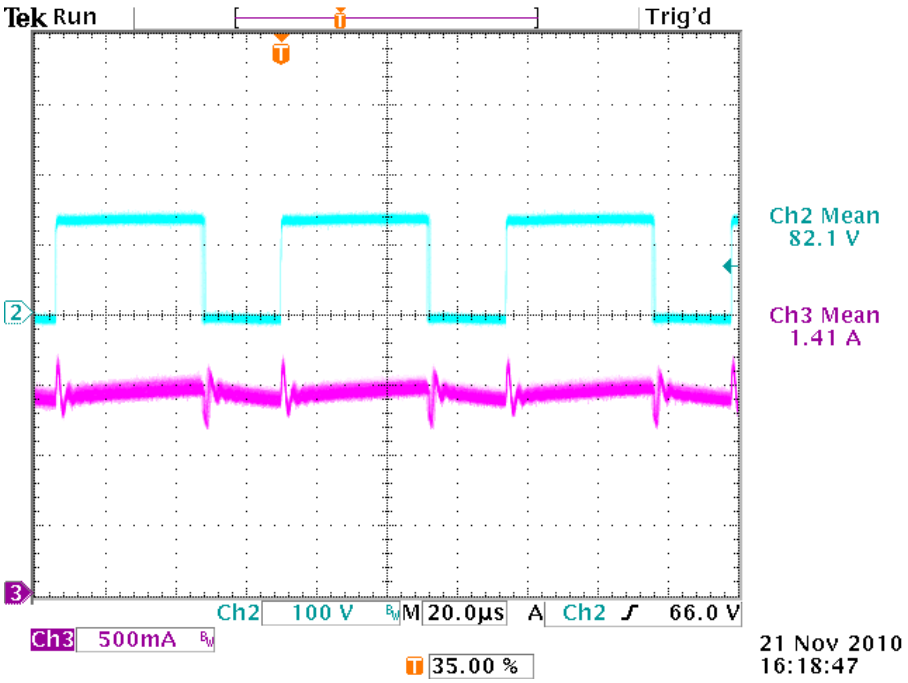

Figure 18. Armature voltage and current at 8 lbf-in commanded and 1300 rpm.

4. Summary of Results

From Table 7, we can see that torque stayed constant because the armature current stays constant regardless of the load or rotor speed. When comparing Figure 15 to Figure 16 and Figure 17 to Figure 18, we can see that the armature current stayed constant at different rotor speeds. As more load torque is applied, the rotor speed and the armature voltage decreased, but the armature current stayed constant at the user commanded torque input value.

D. CHAPTER SUMMARY

In this chapter, two attempts at commanding torque through a Graphical User Interface (GUI) were completed. For the first attempt, the DC motor was controlled by changing armature voltage to control the electric torque. This achieved an output torque to the motor but varied because the calculation relied upon a rotor speed measurement feedback that varied as load on the motor changed. The varying rotor speed caused the applied armature voltage and currents to change, which varied the electric torque output. Finally, the DC motor torque was commanded by controlling the armature current independent of rotor speed. This allowed for a successful user commanded torque to output torque regardless of the rotor speed.

IV. CONCLUSIONS AND FUTURE RESEARCH

A. CONCLUSIONS

In summary, a program that commands torque to a separate-winding excitation DC motor was created, simulated, and tested using standard engineering principles and theory. The program was designed around the theory of separate-winding excitation DC motor operation. A test was conducted that validated how the separate-winding excitation DC motor operates, and then the torque commanding program was built to output the correct desired torque to the DC motor. The final experimental results showed that the system responded according to theory.

With this baseline way to command torque to a DC motor, the Naval Postgraduate School can now apply this concept to command torque to drive other systems such as the DFIG control system [5] or other laboratory research and future work. A profile of behavior of torque versus rotor speed at a given armature voltage for the Labvolt DC motors is also provided. The future research on this topic will be above and beyond current publications and will have an enabled freedom to exploit the abilities of the DC motor.

B. FUTURE RESEARCH

The DC motor can be profiled and programmed for shunt-connected, series-connected, or compound-connected operation. The theory can be studied to profile how the Labvolt DC motor behaves under different operating conditions. The output torque can be commanded in the same manor discussed in this thesis.

Secondly, the commanded torque program can be tested on the DFIG system [5] to test at fixed steady-state defined torque from the DC motor. This should be completed to further validate that torque can be commanded to another system other than a dynamometer.

Third, a Matlab/Simulink programming can be written output random commanded torque from the DC motor. A program written for random torque can be used to simulate random wind input to a DFIG system from [5] or other laboratory research.

APPENDIX A: DATASHEETS

SEMISTACK - IGBT

SEMITRANS Stack[1)]

Three-phase rectifier + inverter with brake chopper

SEMITEACH - IGBT
SKM 50 GB 123D
SKD 51
P3/250F

Features

- Multi-function IGBT converter
- Transparent enclosure to allow visualization of every part
- IP2x protection to minimize safety hazards
- External banana/BNC type connectors for all devices
- Integrated drive unit offering short-circuit detection/cut-off, power supply failure detection, interlock of IGBTs + galvanic isolation of the user
- Forced-air cooled heatsink

Typical Applications

- Education: One stack can simulate almost all existing industrial applications:
- 3-phase inverter+brake chopper
- Buck or boost converter
- Single phase inverter
- Single or 3-phase rectifier

[1)] Photo non-contractual

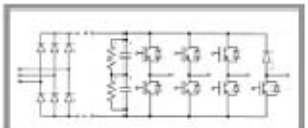

B6U + B6CI + E1CIKF

Circuit	I_{rms} (A)	V_{ac} / V_{dcmax}	Types
B6CI	30	440 / 750	SEMITEACH - IGBT

Symbol	Conditions	Values	Units
I_{rms}	no overload	30	A
	IGBT - 4x SKM 50 GB 123D		
V_{CES}		1200	V
$V_{CE(SAT)}$	I_C= 50A, V_{GE}= 15V, chip level; T_j= 25(125)°C	2,7 (3,5)	V
V_{GES}		±20	V
I_C	T_{case}= 25 (80)°C	50 (40)	A
I_{CM}	T_{case}= 25 (80)°C; t_p= 1ms	100 (80)	A
	Rectifier - 1x SKD 51/14		
$V_{in(max)}$	without filter	3 x 480	V
	with filter	3 x 380	V
	DC Capacitor bank - Electrolytic 2x 2200µF/400V		
C_{eqv}	total equivalent capacitance	1100 / 800	µF / V
V_{DCmax}	max. DC voltage applied to the capacitor bank	750	V
	Driver - 4x SKHI 22		
Power supply		0 / 15	V
Current consumption	max; per driver	16	mA
Thermal trip	Normally Open type (NO)	71	°C

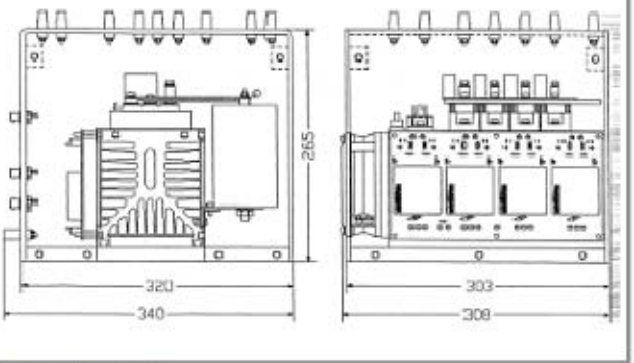

General dimensions

Model 8211 DC Motor/Generator

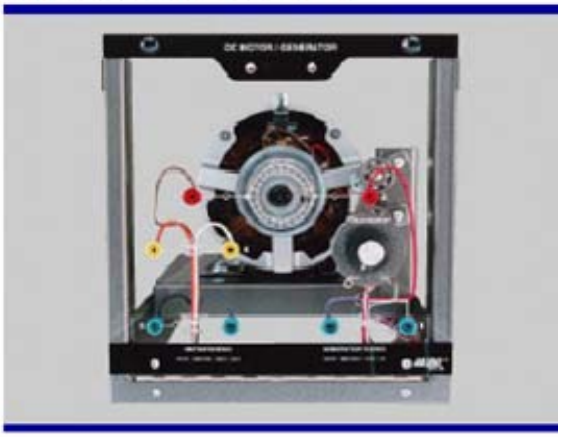

This machine can be run independently as a DC motor or a DC generator. The armature, shunt field, and series field windings are terminated separately on the faceplate to permit long and short shunt as well as cumulatively and differentially compounded motor and generator connections. This machine is fitted with exposed movable brushes to allow students to study the effect of armature reaction and commutation while the machine is operating under load. An independent, circuit-breaker protected, shunt-field rheostat is mounted on the faceplate for motor speed control or generator output voltage adjustment.

SPECIFICATIONS

Model 8211 DC Motor/Generator		120/208 V – 60 Hz	220/380 V – 50 Hz	240/415 V – 50 Hz
Power Requirement		120/208 V	220/380 V	240/415 V
Rating	Motor Output Power	175 W		
	Generator Output Power	120 W	110 W	120 W
	Armature Voltage	120 V – DC	220 V – DC	240 V – DC
	Shunt Field Voltage	120 V – DC	220 V – DC	240 V – DC
	Full Load Speed	1800 r/min	1500 r/min	1500 r/min
	Full Load Motor Current	2.8 A	1.3 A	1.1 A
	Full Load Generator Current	1 A	0.5 A	0.5 A
Physical Characteristics	Dimensions (H x W x D)	308 x 291 x 440 mm (12.1 x 11.5 x 17.3 in)		
	Net Weight	14.1 kg (31 lb)		

Model 8911 – Electrodynamometer

The Model 8911 Electrodynamometer is equipped with a clear plastic faceplate fitted with a chrome piano hinge. It can be coupled to a 0.2-kW drive motor through the use of the Timing Belt (Model 8942). The faceplate can be lowered to provide access to the inside for coupling the Electrodynamometer to the drive motor. When closed, the faceplate is secured by two quick-lock fasteners.

The Electrodynamometer is made of a squirrel-cage rotor fitted in a DC-excited stator. Mechanical loading is achieved by increasing the stator field current, which generates eddy currents in the driven rotor. The stator is trunnion-mounted on ball bearings and rotates against a helicoidal spring to oppose braking torque. The front end bell is provided with a circular scale that indicates the torque developed. The circular scale is graduated in either Imperial units (lbf·in, Model 8911) or Metric units (N·m, Model 8911-1) depending on model numbers. The Electrodynamometer is electrically powered from standard fixed AC line supply.

SPECIFICATIONS

Model 8911 Electrodynamometer		120/208 V – 60 Hz	220/380 V – 50 Hz	240/415 V – 50 Hz
Rating	Torque Range (8911-1)	-0.3 to +3 N·m		
	Torque Range (8911)	-3 to +27 lbf·in		
	Speed	250 to 3000 r/min		
	Accuracy	2%		
	Input Voltage	120 V – AC	220-240 V – AC	
	Input Current	2 A	0.9 A	
Physical Characteristics	Dimensions (H x W x D)	308 x 291 x 490 mm (12.1 x 11.5 x 19.3 in)		
	Net Weight	17.4 kg (38.3 lb)		

POWER SUPPLY
MODEL 8821

The Power Supply provides fixed and variable AC and DC voltage sources, all terminated by color-coded 4 mm safety sockets. Independent circuit breakers, reset at the front panel, protect the input to and output from the Power Supply. Indicator lamps monitor the presence of input voltage in each phase. When a phase leg of the site's power service is out, the lamp goes off to reflect this condition.

A voltmeter, connected through a selector switch, monitors the variable AC and DC outputs and fixed DC output. A 24 V AC output provides a low-voltage supply required to operate other EMS equipment such as metering modules and modules used in the Power Electronics Training System.

SPECIFICATIONS

Model 8821 – Power Supply		120/208 V – 60 Hz	220/380 V – 50 Hz	240/415 V – 50 Hz
Input	Line Voltage	120/208 V	220/380 V	240/415 V
	Line Current	15 A	10 A	
	Service Installation	20 A, 3-phase, 5 wires, star (Wye)- connected, including neutral and ground		
Outputs	Fixed AC 3-Phase	120/208 V – 15 A	220/380 V – 10 A	240/415 V – 10 A
	Variable AC 3-Phase	0-120/208 V – 5 A	0-220/380 V – 3 A	0-240/415 V – 3 A
	Variable DC	0-120 V – 8 A	0-220 V – 5 A	0-240 V – 5 A
	Fixed DC	120 V – 2 A	220 V – 1 A	240 V – 1 A
	Low Power AC	24 V – 3 A		
Wall Outlet included		NEMA L21-20	NEMA L22-20	CLIPSAL 56SO520
Power Cord		3 m (10 ft)		
Physical Characteristics	Dimensions (H x W x D)	308 x 287 x 500 mm (12.1 x 11.3 x 19.7 in)		
	Net Weight	10.4 kg (40.5 lb)		

ME-20-P series

[Square Wave/Incremental]

Outside dimensions

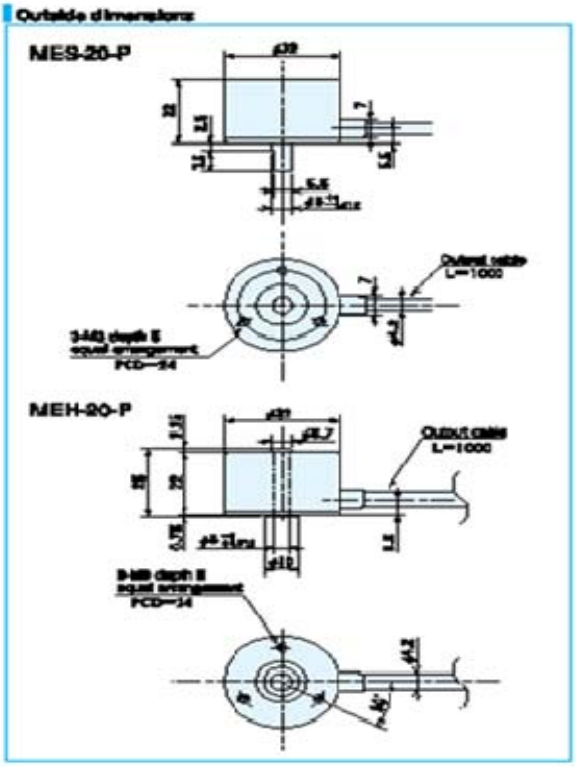

Specifications

Item			
Type name	ME□-20-□P□		
Supply voltage	DC5—12V ±10% DC24V±10% (open collector output only)		
Current consumption	60mA or less (under no load)		
Detection system	Incremental		
Output pulse number (P/revolution) (Pulse number/revolution)	50 100 200 250 360 250 500 1000 1024 1800 500 1000 2048 2500 3600 1000 2000 4096 5000 7200		
Output phase	A, B, Z phase		
Output form	Square wave		
Output capacity	Sink current: 20mA Residual voltage: 0.5V or less (at 15mA)		
Maximum response frequency (response pulse width)	100kHz		
Output phase difference	A, B phase difference 90°±45° (T/4±T/8) Z phase T±T/2 (one Output Waveform)		
Waveform rise/fall time	1μs or less (output cable 1m or less)		
Starting torque	20×10⁻³N·m (20gf·cm) or less		
Allowable load of shaft (Reference)	Radial	19.6N (2kgf)	14.7N (1.5kgf)
	Thrust	9.8N (1kgf)	4.9N (0.5kgf)
Maximum allowable revolution	6,000rev/min		
Starting ambient temperature	-10°C—70°C (No dewing)		
Storing ambient temperature	-20°C—80°C		
Vibration resistance	Durability 55Hz, double amplitude 1.5mm 2 hours each in X, Y, and Z directions		
Impact resistance	Durability 200m/s² (about 20G) 3 times each in X, Y, and Z directions		
Cable	Outside diameter φ4.2 5-core vinyl-wire Twisted shield cable (length 1m)		
Mass	70g		

Output circuit diagram

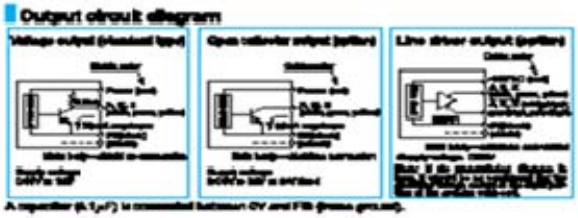

A capacitor (0.1μF) is connected between 0V and FG (frame ground).

Output waveform

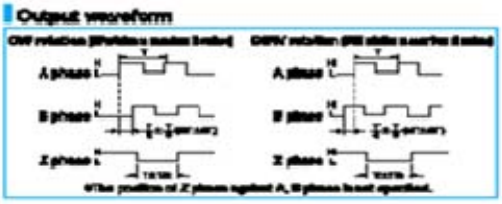

Specifications/Sine wave

Supply voltage		DC5V ±5%
Current consumption		40mA or less (under no load)
Detection system		Sine wave•incremental
Output	Output pulse number (Standard) (Pulse number/rotation)	1,000 2,000 2,500
	Output phase	A, B, Z phase
	Output form	A, B phase SIN wave, Z phase square wave
	A, B, Z phase output	SIN wave 1.5 Vp-p±0.3 V offset: 2.0V±0.2V
		Opamp output current 5mA Max.
		Harmonic distortion factor to be within 10% (Measuring condition to be within 20 kHz, effective value mean distortion factor measuring instrument)
	Maximum response frequency	50kHz
	Output phase difference	A, B phase difference 90°±45° (T/4±T/8) Z phase T±T/2 (see Output Waveform)
Starting torque		2×10⁻³N•m (20gf•cm) or less
Allowable load of shaft (electrical)	Radial	14.7N (1.5kgf)
	Thrust	4.9N (0.5kgf)
Maximum allowable revolutions (mechanical)		6,000r/min
Working ambient temperature/ humidity		0°C~50°C RH35%~90% no dewing
Storing ambient temperature		−20°C~80°C
Vibration resistance		Durability 55Hz, double amplitude 1.5mm 2 hours each in X, Y, and Z directions
Impact resistance		Durability 500m/s² (about 50G) 3 times each in X, Y, and Z directions
Cable		Outside diameter φ4.2 5-core vinyl wire Insulated shield cable (length 1m)
Mass		70g

Output circuit diagram

Sine wave output (option)

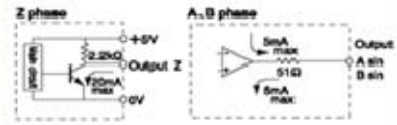

Signal name	Lead wire color
Vcc	Red
0V	Black
A phase	White
B phase	Green
Z phase	Yellow

A capacitor (0.1μF) is connected between 0V and FG (frame ground).

Output waveform

Sine wave output (option)
CW rotation (CW rotation as seen from ft surface)

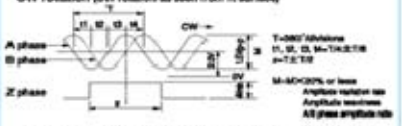

*The position of Z phase against A, B phase is not specified.

Specifications Built-in multiplication circuit (×2•×4•×8•×16)

Supply voltage		Voltage/Open collector:DC5V±5%~12V±10% Line driver:DC5V±5%
Current consumption		60mA or less (under no load)
Detection system		Incremental
Output	Output pulse number (Standard) (Pulse number/rotation)	EX 2,500×2 (5,000) 2,500×4 (10,000) 2,500×8 (20,000) 2,500×16 (40,000)
	Output phase	A, B, Z phase
	Output form	Square wave
	Output capacity	Open collector out put:load voltage DC13.2V max
	Maximum response frequency	Line driver output:50kHz×× (by multiplication) Voltage output•Open collector output:100kHz
	Output phase difference	See the diagram below.
Starting torque		2×10⁻³N•m (20gf•cm) or less
Allowable load of shaft (electrical)	Radial	14.7N (1.5kgf)
	Thrust	4.9N (0.5kgf)
Maximum allowable revolutions (mechanical)		6,000r/min
Working ambient temperature/ humidity		−10°C~70°C RH35%~90% no dewing
Storing ambient temperature		−20°C~80°C
Vibration resistance		Durability 55Hz, double amplitude 1.5mm 2 hours each in X, Y, and Z directions
Impact resistance		Durability 500m/s² (about 50G) 3 times each in X, Y, and Z directions
Cable		Outside diameter φ4.2 5-core vinyl wire Insulated shield cable (length 1m)
Mass		70g

Output circuit diagram

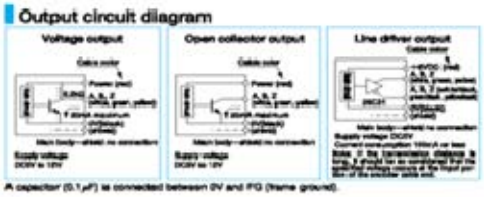

A capacitor (0.1μF) is connected between 0V and FG (frame ground).

Output waveform

CW rotation (CW rotation as seen from ft surface)

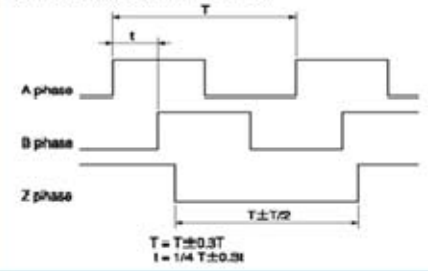

T = T±0.3T
t = 1/4 T±0.3t

14

APPENDIX B: MATLAB M-FILES

A. MATLAB INITIAL CONDITIONS FILE

Derges_ic.m

```
open_loop=0 ;         %Set to one for open loop operation else set to
zero for closed loop voltage regulation
Kp_i=.06*2;     %current PI gain is amplified to account for the SV
modulation scaling
Ki_i=1*3;    %Current control loop gain
Kp_v=.2;
Ki_v=1.5;
f_clock=24e6;
sw_freq=15000;
sw_counter=round(f_clock/sw_freq-mod(f_clock/sw_freq,10));      %Counter
for sawtooth for switching modulo 10 used so step_ct can be 10
Vdc=48;
oversample=4;  %1 4 work
fin=100;
Kv=0.6;
ra=8.5;



%step_ct=10;
step_ct=1;
tstep = step_ct/f_clock;
F_mat = [0 0 0 1;1 1 2 0;2 2 3 0;3 3 0 0];
O_mat = F_mat;

%%%%%%%%%%%%%%%%%%Encoder                                          Speed
Vector%%%%%%%%%%%%%%%%%%%%%%%%%%%%%%%%%%%%%%%%%
Index1=[1:2^12];
reciprocal1=2^-6./Index1;

%%%%%%%%%%%%%%%%%%Encoder
Vector%%%%%%%%%%%%%%%%%%%%%%%%%%%%%%%%%%%%%%%%%%%%%%%
output_vec1=[0;...
            0;...
            2;...%Motor is turning in the CCW falling edge
            1;...%Motor is turning in the CW falling edge
            1;...%Motor is turning in the CW rising edge
            2;...%Motor is turning in the CCW rising edge
            0;...
            0];
%%%%%%%%%%%%%%%%%%%%%%%%%%%%%%%%%%%%%%%%%%%%%%%%%%%%%%%%%%%%%%%%%%%%%%%%%%%%
%%%%
```

B. MATLAB FILE USED FOR RAMP IN

ramp2mod.m

```
function z = ramp2(x)
gain=xfix({xlSigned,20,19},1/1602)
z=xfix({xlSigned,14,13},x*gain);
```

C. MATLAB M-FILES FOR CHIPSCOPE INTERFACE

Black_box_dc_machine2_config.m

```
function code_config(this_block)

  % Revision History:
  %
  %   01-Nov-2010  (11:34 hours):
  %         Original code was machine generated by Xilinx's System
Generator after parsing
  %     C:\Derges\black_box_wspeed.vhd
  %
  %

  this_block.setTopLevelLanguage('VHDL');

  this_block.setEntityName('code');

  % System Generator has to assume that your entity    has a
combinational feed through;
  %   if it  doesn't, then comment out the following line:
  this_block.tagAsCombinational;

  this_block.addSimulinkInport('ind');
  this_block.addSimulinkInport('speedin');
  this_block.addSimulinkInport('dcvolts');
  this_block.addSimulinkInport('ila_clock');
  this_block.addSimulinkInport('ind2');

  this_block.addSimulinkOutport('outd');
  this_block.addSimulinkOutport('open_loop');
  this_block.addSimulinkOutport('torque_lbf_in');
  this_block.addSimulinkOutport('load_duty');

  outd_port = this_block.port('outd');
  outd_port.setType('UFix_1_0');
  open_loop_port = this_block.port('open_loop');
  open_loop_port.setType('UFix_1_0');
  torque_lbf_in_port = this_block.port('torque_lbf_in');
  torque_lbf_in_port.setType('UFix_8_0');
  load_duty_port = this_block.port('load_duty');
  load_duty_port.setType('UFix_8_0');
```

```
  % ------------------------------
  if (this_block.inputTypesKnown)
    % do input type checking, dynamic output type and generic setup in
this code block.

    if (this_block.port('ind').width ~= 1);
      this_block.setError('Input data type for port "ind" must have
width=1.');
    end

    if (this_block.port('speedin').width ~= 12);
      this_block.setError('Input data type for port "speedin" must have
width=12.');
    end

    if (this_block.port('dcvolts').width ~= 8);
      this_block.setError('Input data type for port "dcvolts" must have
width=8.');
    end

    if (this_block.port('ila_clock').width ~= 1);
      this_block.setError('Input data type for port "ila_clock" must
have width=1.');
    end

    this_block.port('ila_clock').useHDLVector(false);

    if (this_block.port('ind2').width ~= 48);
      this_block.setError('Input data type for port "ind2" must have
width=48.');
    end

  end  % if(inputTypesKnown)
  % ------------------------------

  % ------------------------------
   if (this_block.inputRatesKnown)
     setup_as_single_rate(this_block,'clk','ce')
   end  % if(inputRatesKnown)
  % ------------------------------

    % (!) Set the inout port rate to be the same as the first input
    %     rate. Change the following code if this is untrue.
    uniqueInputRates = unique(this_block.getInputRates);


  % Add addtional source files as needed.
  %  |-------------
  %  | Add files in the order in which they should be compiled.
  %  | If two files "a.vhd" and "b.vhd" contain the entities
  %  | entity_a and entity_b, and entity_a contains a
  %  | component of type entity_b, the correct sequence of
  %  | addFile() calls would be:
```

```
  %  |    this_block.addFile('b.vhd');
  %  |    this_block.addFile('a.vhd');
  %  |-------------

  %    this_block.addFile('');
  %    this_block.addFile('');
  this_block.addFile('black_box_wspeed.vhd');

return;


% ------------------------------------------------------------

function setup_as_single_rate(block,clkname,cename)
  inputRates = block.inputRates;
  uniqueInputRates = unique(inputRates);
  if (length(uniqueInputRates)==1 & uniqueInputRates(1)==Inf)
    block.addError('The inputs to this block cannot all be constant.');
    return;
  end
  if (uniqueInputRates(end) == Inf)
     hasConstantInput = true;
     uniqueInputRates = uniqueInputRates(1:end-1);
  end
  if (length(uniqueInputRates) ~= 1)
    block.addError('The inputs to this block must run at a single
rate.');
    return;
  end
  theInputRate = uniqueInputRates(1);
  for i = 1:block.numSimulinkOutports
     block.outport(i).setRate(theInputRate);
  end
  block.addClkCEPair(clkname,cename,theInputRate);
  return;

% ------------------------------------------------------------
```

APPENDIX C: SIMULINK/XILINX MODEL OF COMMAND TORQUE, CURRENT CONTROLLED DC MOTOR

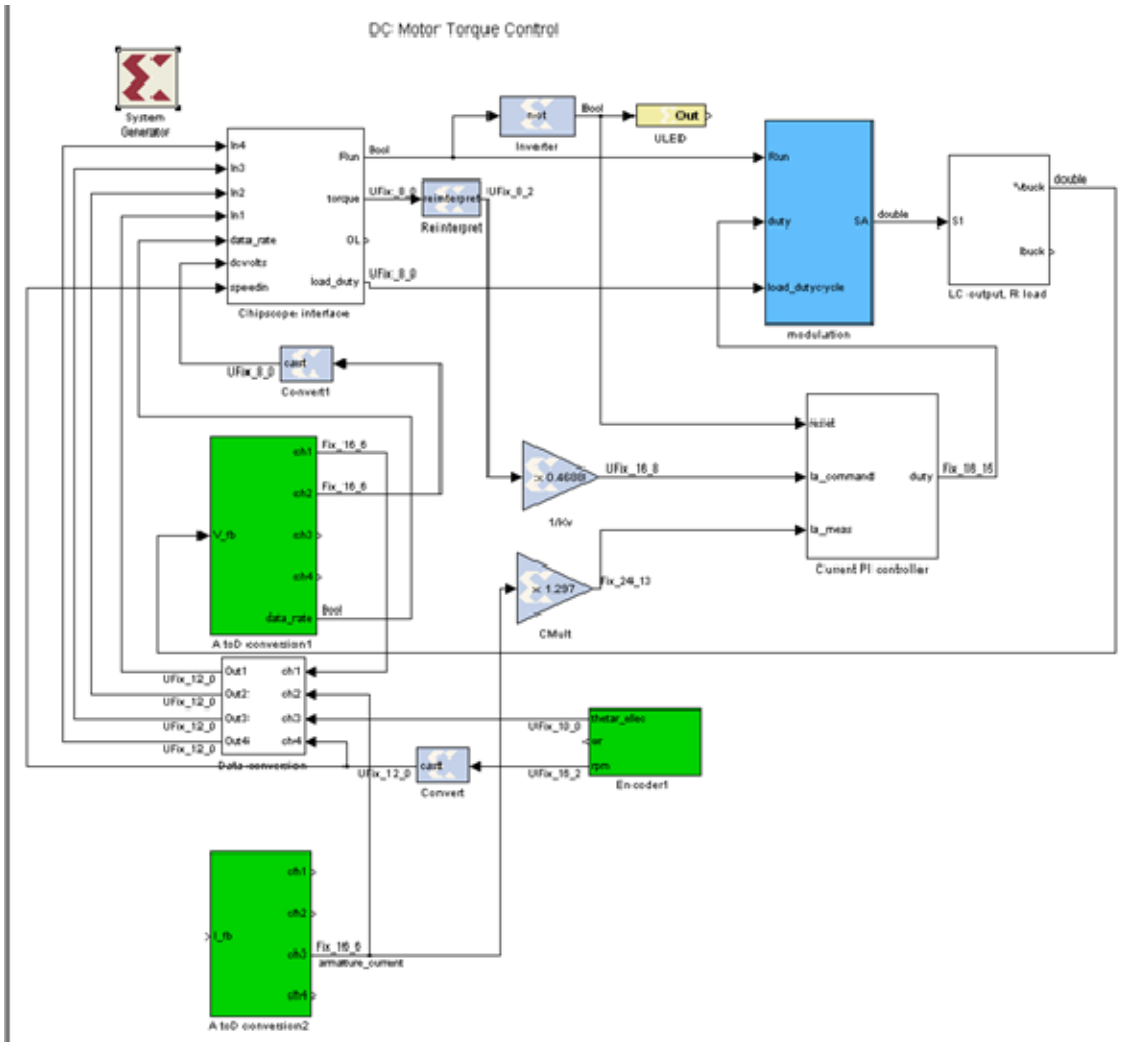

Figure 19. Overall system.

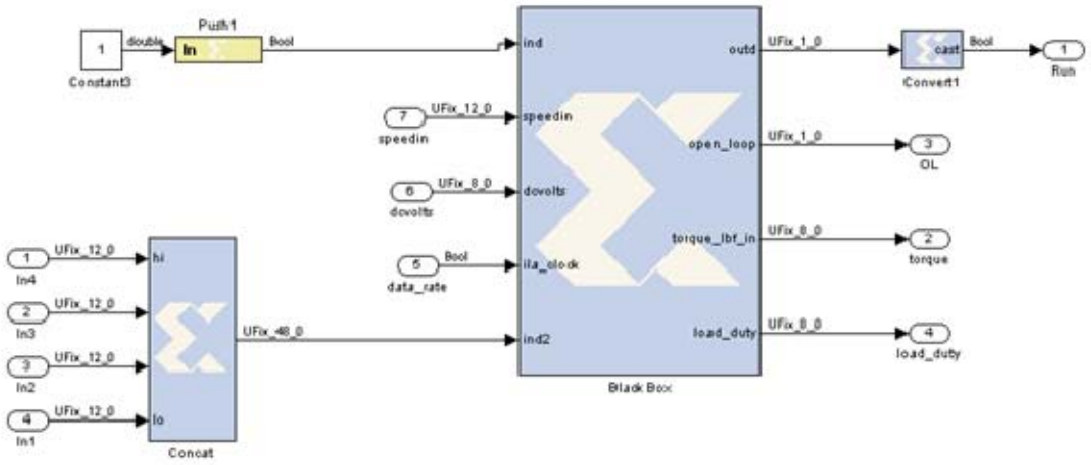

Figure 20. Chipscope interface.

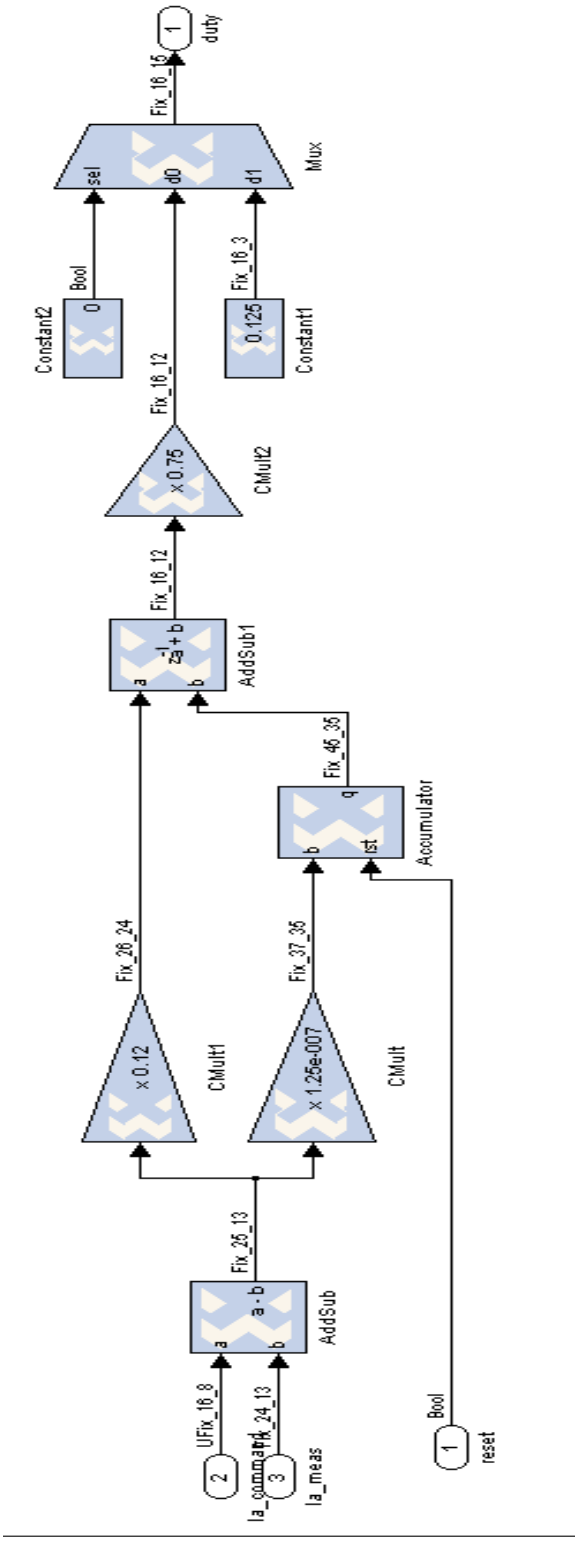

Figure 21. Current PI controller.

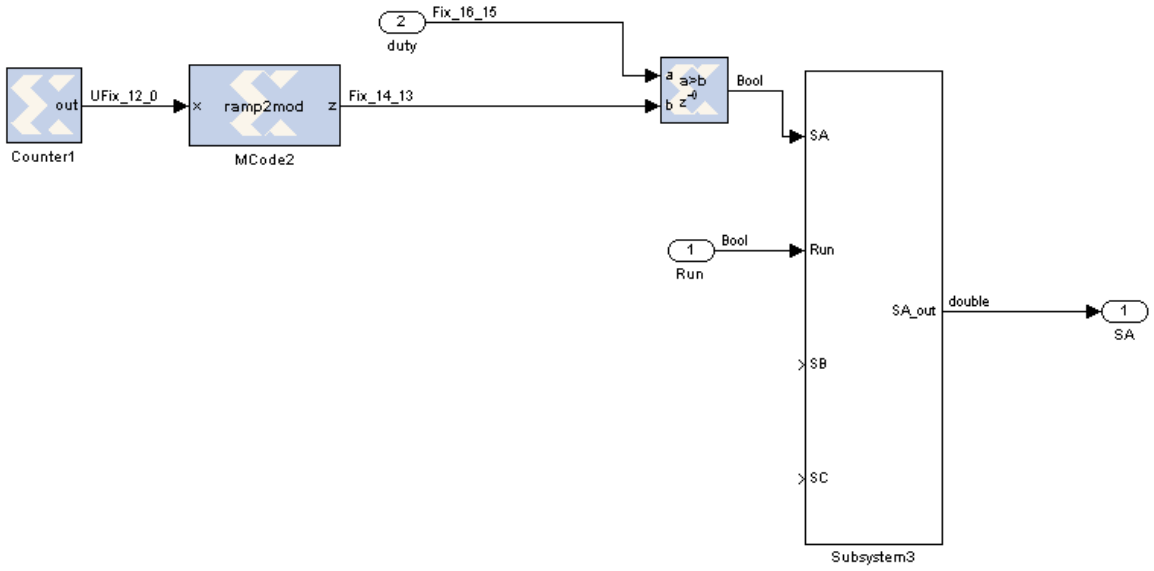

Figure 22. Modulation.

Figure 23. Subsystem3 from modulation.

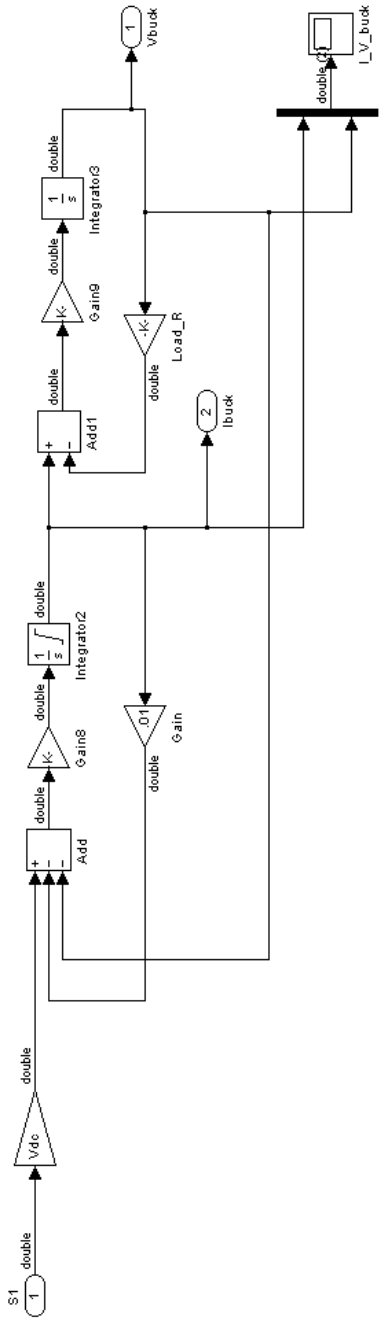

Figure 24. LC output, R lead.

THIS PAGE INTENTIONALLY LEFT BLANK

APPENDIX D: COMMANDED TORQUE HEXADECIMAL INPUT

Torque (lbf-in)	Hexadecimal Input		Torque (lbf-in)	Hexadecimal Input
0	00		6.75	1B
0.25	01		7.0	1C
0.5	02		7.25	1D
0.75	03		7.5	1E
1.0	04		7.75	1F
1.25	05		8.0	20
1.5	06		8.25	21
1.75	07		8.5	22
2.0	08		8.75	23
2.25	09		9.0	24
2.5	0A		9.25	25
2.75	0B		9.5	26
3.0	0C		9.75	27
3.25	0D		10.0	28
3.5	0E		10.25	29
3.75	0F		10.5	2A
4.0	10		10.75	2B
4.25	11		11.0	2C
4.5	12		11.25	2D
4.75	13		11.5	2E
5.0	14		11.75	2F
5.25	15		12.0	30
5.5	16		12.25	31
5.75	17		12.5	32
6.0	18		12.75	33
6.25	19		13.0	34
6.5	1A		13.25	35

Torque (lbf-in)	Hexadecimal Input		Torque (lbf-in)	Hexadecimal Input
13.5	36		17.0	44
13.75	37		17.25	45
14.0	38		17.5	46
14.25	39		17.75	47
14.5	3A		18.0	48
14.75	3B		18.25	49
15.0	3C		18.5	4A
15.25	3D		18.75	4B
15.5	3E		19.0	4C
15.75	3F		19.25	4D
16.0	40		19.5	4E
16.25	41		19.75	4F
16.5	42		20.0	4G
16.75	43			

LIST OF REFERENCES

[1] "Defense infrastructure: Department of Defense renewable energy initiatives," *Briefing for the Committees on Armed Services, United States Senate and House of Representatives.* Government Accountability Office, 26 April 2010.

[2] Lucy Y. Pao, Kathryn E. Johnson, "A Tutorial on the Dynamics and Control of Wind Turbines and Wind Farms," *American Control Conference, 2009, ACC '09,* St. Louis, MO, pages 2076–2089, 2009.

[3] Gregory W. Edwards, "Wind Power Generation Emulation via Doubly-Fed Induction Generator Control," Master's Thesis, Naval Postgraduate School, 2009.

[4] S. Muller, M. Deicke, and Rik W. de Doncker (2002 May/June). Doubly Fed Induction Generator Systems for Wind Turbines. *IEEE Inductry Applications Magizine*, 26–33, 2002.

[5] Paul C. Krause, Oleg Wasynczuk, and Scott D. Sudhoff. "Analysis of Electric Machinery and Drive Systems," John Wiley & Sons, Inc., 2002.

[6] Alexander. L. Julian, Notes for EC4130 (Advanced Electrical Machinery Systems), Naval Postgraduate School, 2007 (unpublished).

[7] Alexander L. Julian, Laboratory for EC3130 (Electrical Machinery Systems), "Speed control of a DC Motor with Varying Load," Naval Postgraduate School, 2010 (unpublished).

[8] Joseph E. O'Connor, "Field Programmable Gate Array Control of Power Systems in Graduate Student Laboratories," Master's Thesis, Naval Postgraduate School, 2008.

[9] Ned Mohan, Tore M. Undeland, William P. Robbins, "Power Electronics," John Wiley & Sons, Inc., 2003.

THIS PAGE INTENTIONALLY LEFT BLANK

INITIAL DISTRIBUTION LIST

1. Defense Technical Information Center
   Ft. Belvoir, Virginia

2. Dudley Knox Library
   Naval Postgraduate School
   Monterey, California

3. Dr. R. Clark Roberson
   Navy Postgraduate School
   Monterey, California

4. Dr. Alexander L. Julian
   Navy Postgraduate School
   Monterey, California

5. Dr. Roberto Cristi
   Naval Postgraduate School
   Monterey, California

6. LT Jonathan Derges, USN
   SUPSHIP Newport News
   Newport News, Virginia